Modern Journal of Statistics
2(2), 103–128
DOI:https://doi.org/10.64389/mjs.2026.02275
https://sphinxsp.org/journal/index.php/mjs/

Research article

Topp-Leone Reduced Kies Distribution for Unit-Interval Data: Statistical Properties, Parameter Estimation, and Applications

Ehinomen Emmanuel Ehizojie *

Department of Statistics, Faculty of Physical Sciences, Ahmadu Bello University, Zaria 810211, Nigeria

* **Correspondence:** ehizojieee@gmail.com

ARTICLE INFO

Keywords:
Topp-Leone-G family of distributions
Reduced kies distribution
Monte Carlo simulation
Percentile-based Estimation
Cramér-von Mises

Mathematics Subject Classification:
60E05, 62E15, 62F10

Important Dates:
Received: 12 March 2026
Revised: 6 May 2026
Accepted: 4 June 2026
Online: 17 June 2026

ABSTRACT

This study introduces a two-parameter lifetime model named the Topp-Leone Reduced Kies (TLRK) distribution, which extends the Topp-Leone-G family by incorporating the Reduced Kies (RK) distribution as its baseline. The proposed distribution is designed for unit-interval data, such as proportions, rates, and reliability metrics. The TLRK distribution exhibits left-skewed, right-skewed, decreasing (or L-shaped), bathtub-shaped, and near-symmetric shaped density while the hazard rate function exhibits an increasing, and bathtub-shaped failure rates behaviour. Several statistical properties of the TLRK distribution, including moments, moment generating function, Rényi entropy, and order statistics are investigated. Seven distinct parameter estimation methods namely maximum likelihood, least squares, Cramér-von Mises, maximum product of spacings, Anderson-Darling, weighted least squares, and percentile-based estimation; are implemented and compared. A Monte Carlo simulation study evaluates the finite-sample performance of these estimators across varying sample sizes. The practical utility of the TLRK distribution is demonstrated through the analysis of two real unit-interval datasets (failure times of Kevlar strands and relief times of arthritic patients). Comparative analysis indicates that the TLRK distribution shows a favourable fit relative to some existing RK-based models, including the Reduced Kies, Extended Reduced Kies, Exponential Reduced Kies, and Marshall-Olkin Reduced Kies distributions.

1. Introduction

The construction of flexible probability distributions remains a fundamental objective in statistical modelling, particularly in the analysis of lifetime, reliability, and bounded data. Classical distributions often prove inadequate for capturing complex empirical features such as skewness, heavy tails, and non-monotonic hazard rate behaviour. Consequently, a widely adopted approach involves extending baseline distributions through generator mechanisms or transformation techniques, thereby enhancing their flexibility and improving their ability to model real data [35].

Several generator families have been proposed in the literature to address these challenges. Notable examples include the Exponential-G family [18], Beta-G family [16], Gamma-G family [39], Kumaraswamy-G family [12], Weibull-G family [10], Odd Lomax Trigonometric-G family [7], Lomax-G family [30], Odd Beta prime-G family [33], Topp-Leone Odd Fréchet-G family [36], Cosine Kumaraswamy-G family [20], and the hybrid cosine inverse Lomax-G family [9]. These advances highlight the growing interest in constructing distributions that can accommodate intricate distributional shapes and diverse hazard rate structures. These families provide a framework for extending classical distributions (such as Beta, Exponential, Rayleigh, Topp-Leone, Gompertz, Fréchet and Weibull) to model more complex data patterns. Thus, these advances highlight the growing interest in constructing distributions that can accommodate intricate distributional shapes and diverse hazard rate structures.

The Reduced Kies (RK) distribution, first introduced by [25], has gained recognition as a versatile lifetime model for data confined to the unit interval (0, 1). This distribution is particularly effective in modelling failure times, reliability data, and other bounded observations, such as percentages, proportions, ratios, and rates. As a single-parameter continuous probability distribution, the RK model constitutes a specialized case of the classical Kies distribution [24], offering a more parsimonious yet flexible alternative for analysing interval-constrained datasets. The cumulative distribution function (CDF) and the probability density function (PDF) of the RK Distribution are respectively expressed as follows:

$$G(x) = 1 - e^{-\left(\frac{x}{1-x}\right)^{\alpha}}, \qquad x \in (0,1), \alpha > 0 \tag{1.1}$$

and

$$g(x) = \alpha x^{\alpha-1}(1-x)^{-\alpha-1} e^{-\left(\frac{x}{1-x}\right)^{\alpha}}, \tag{1.2}$$

where α is a shape parameter.

In recent years, substantial advancements have been made in the characterization and inferential analysis of the Reduced Kies (RK) distribution, as evidenced by key contributions from [13], [37], [4], [1], [8], and [28], among others. These studies have expanded the theoretical foundations and practical applications of the RK distribution.

As a parsimonious single-parameter model, the RK distribution has been extended in various directions to improve its flexibility. These include the Marshall-Olkin Reduced Kies distribution [2], Exponential Reduced Kies distribution [26], Extended Reduced Kies distribution [5], Kumaraswamy Reduced Kies distribution [19], Exponentiated Generalized Reduced Kies distribution [14], and the Alpha Power Reduced Kies distribution [15], among others.

Despite these developments, recent research has identified critical limitations in existing RK extensions, particularly in their ability to simultaneously capture extreme skewness and complex hazard rate behaviours within the unit interval [19]. This gap emphasizes the need for a more flexible distribution capable of capturing extreme asymmetry and varying modal structures in bounded data.

To address this specific gap, we propose the Topp-Leone Reduced Kies (TLRK) distribution. The mathematical novelty lies in the introduction of a second shape parameter β via the Topp-Leone-G transformation, which separates the control of distributional shape from the baseline hazard structure. Specifically, the baseline RK parameter α governs the hazard rate behaviour (increasing or bathtub-shaped), while the additional parameter β independently controls the density's skewness and tail weight. Hence, this leads to improved flexibility in capturing a wide range of distributional shapes, including pronounced skewness, varying tail weights and complex hazard rate patterns. Furthermore, the proposed model retains analytical tractability, with explicit expressions for key statistical properties, thereby facilitating efficient estimation and practical implementation. These features collectively distinguish the TLRK distribution from some existing RK-based models and establish its contribution as both structurally and inferentially meaningful.

The main contributions of this study are summarised as follows. First, a new bounded distribution is derived through a generator-based transformation of the RK model. Second, important statistical properties, including moments, quantile function, moment generating function, entropy, and quartiles measures, are obtained in tractable forms. Third, multiple parameter estimation methods are developed and comparatively evaluated through a Monte Carlo simulation study. Finally, the practical applicability of the proposed model is demonstrated using two real datasets, where its performance is assessed against competing models using well-known discrimination criteria and goodness-of-fit measures.

The remainder of the paper is organised as follows. Section 2 introduces the TLRK distribution and its fundamental functions. Section 3 presents its statistical properties. Section 4 develops parameter estimation procedures. Section 5 reports the results of the simulation study. Section 6 demonstrates the TLRK model's practical flexibility through empirical analysis of two real unit-interval datasets: failure times of Kevlar 49/epoxy strands and relief times of arthritic patients. Finally, Section 7 concludes with a discussion of the findings, limitations, and directions for future research.

2. The Topp-Leone Reduced Kies Distribution

This section introduces the Topp-Leone Reduced Kies (TLRK) distribution using the idea of Topp-Leone-G (TL-G) family of distributions introduced by [3]. If X is a continuous random variable with CDF $G(x)$, then the TL-G family of distributions, $F(x)$ has the CDF and PDF defined respectively as:

$$F(x) = [G(x)]^{\beta}[2 - G(x)]^{\beta} = \left[1 - \left(\bar{G}(x)\right)^2\right]^{\beta}, \qquad x \in \Re,\ \beta > 0 \tag{2.1}$$

and

$$f(x) = 2\beta g(x)\bar{G}(x)[G(x)]^{\beta-1}[2 - G(x)]^{\beta-1} = 2\beta g(x)\bar{G}(x)\left[1 - \left(\bar{G}(x)\right)^2\right]^{\beta-1}, \tag{2.2}$$

where $G(x)$ and $g(x)$ denote the CDF and PDF of the baseline distribution, respectively; and $\bar{G}(x) = 1 - G(x)$.

The CDF and PDF of TLRK distribution are derived by inserting Equation (1.1) into (2.1); and Equations (1.1) and (1.2) into (2.2) respectively, as follows:

$$F(x) = \left[1 - \left(1 - \left\{1 - e^{-\left(\frac{x}{1-x}\right)^{\alpha}}\right\}\right)^2\right]^{\beta} = \left[1 - \left(e^{-\left(\frac{x}{1-x}\right)^{\alpha}}\right)^2\right]^{\beta} = \left[1 - e^{-2\left(\frac{x}{1-x}\right)^{\alpha}}\right]^{\beta} \tag{2.3}$$

and

$$f(x) = 2\beta\left(\alpha x^{\alpha-1}(1-x)^{-\alpha-1}e^{-\left(\frac{x}{1-x}\right)^{\alpha}}\right)\left(1 - \left(1 - e^{-\left(\frac{x}{1-x}\right)^{\alpha}}\right)\right)\left[1 - \left(1 - \left(1 - e^{-\left(\frac{x}{1-x}\right)^{\alpha}}\right)\right)^2\right]^{\beta-1}$$

$$= 2\alpha\beta x^{\alpha-1}(1-x)^{-\alpha-1}\left(e^{-\left(\frac{x}{1-x}\right)^{\alpha}}\right)\left(e^{-\left(\frac{x}{1-x}\right)^{\alpha}}\right)\left[1-\left(e^{-\left(\frac{x}{1-x}\right)^{\alpha}}\right)^{2}\right]^{\beta-1}$$

$$= 2\alpha\beta x^{\alpha-1}(1-x)^{-\alpha-1}e^{-2\left(\frac{x}{1-x}\right)^{\alpha}}\left[1-e^{-2\left(\frac{x}{1-x}\right)^{\alpha}}\right]^{\beta-1}, \tag{2.4}$$

where: $0 < x < 1$; $\alpha > 0$ and $\beta > 0$ are shape parameters, respectively.

Figure 1 illustrates the varied forms of the PDF of the TLRK distribution under specific parameter configurations. It is evident that the TLRK distribution exhibits a range of profiles, including unimodal, left-skewed or right-skewed, decreasing (or L-shaped), bathtub-shaped, and near-symmetric shapes. Specifically, $(\alpha = 0.1, \beta = 1.5)$ represents the bathtub-shaped (U-shaped) regime; $(\alpha = 0.4, \beta = 1.5)$ the monotonically non-increasing (L-shaped) regime; $(\alpha = 0.7, \beta = 1.4)$ the decreasing regime; $(\alpha = 0.7, \beta = 2.2)$ the right-skewed unimodal regime; $(\alpha = 0.7, \beta = 4.5)$ the left-skewed unimodal regime; and $(\alpha = 2.5, \beta = 1.5)$ the near symmetric regime. This versatility indicates that the TLRK distribution holds significant promise for modelling datasets within the unit interval across a wide array of applied disciplines.

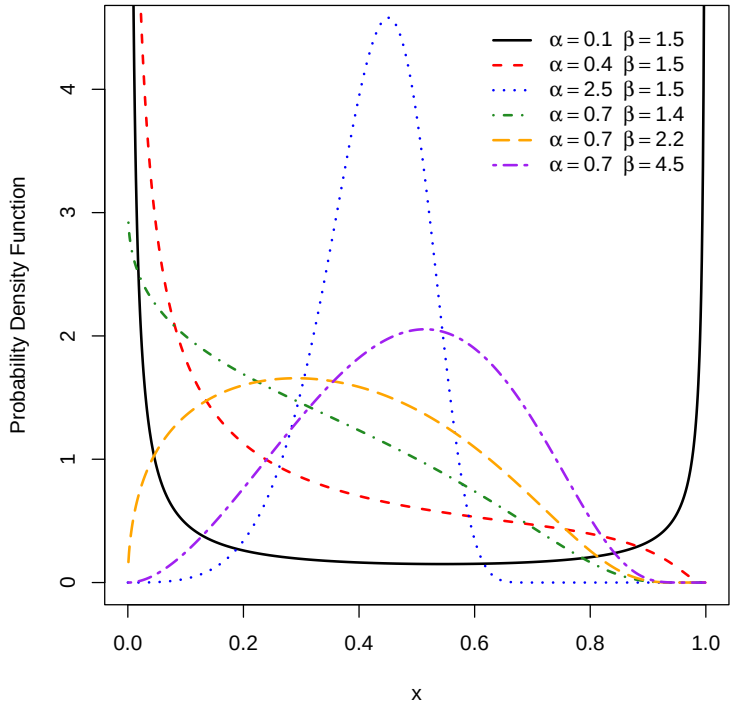

Figure 1. The PDF plots of TLRK distribution.

2.1. The Survival and Hazard Rate Functions

In survival analysis and reliability engineering, the survival function (SF), denoted by $S(x)$, represents the probability that a system or individual survives beyond time x. It is defined as $S(x) = 1 - F(x)$, where $F(x)$ is the CDF. The hazard rate function (HRF), denoted by $h(x)$, describes the instantaneous failure rate at time x given survival up to that time, and is defined as $h(x) = f(x)/S(x)$. These functions are fundamental characterisations of lifetime distributions and provide insights into failure patterns over time.

For the TLRK distribution, the SF and HRF are respectively given as:

$$S(x) = 1 - \left[1 - e^{-2\left(\frac{x}{1-x}\right)^{\alpha}}\right]^{\beta} \tag{2.5}$$

and

$$h(x) = \frac{2\alpha\beta x^{\alpha-1}(1-x)^{-\alpha-1} e^{-2\left(\frac{x}{1-x}\right)^{\alpha}}\left[1 - e^{-2\left(\frac{x}{1-x}\right)^{\alpha}}\right]^{\beta-1}}{1 - \left[1 - e^{-2\left(\frac{x}{1-x}\right)^{\alpha}}\right]^{\beta}}. \tag{2.6}$$

Figure 2 depicts the graphical characteristics of the HRF of the TLRK distribution under some selected parameter settings. The HRF exhibits considerable flexibility, including increasing and bathtub-shaped behaviours. At $(\alpha = 0.1, \beta = 1.5)$ and $(\alpha = 0.4, \beta = 1.5)$ exhibit the bathtub-shaped (U-shaped) behaviour; while $(\alpha = 0.7, \beta = 1.4)$, $(\alpha = 0.7, \beta = 2.2)$, $(\alpha = 0.7, \beta = 4.5)$ and $(\alpha = 2.5, \beta = 1.5)$ exhibit an increasing failure rates behaviour, respectively. The bathtub shape indicates an initial period of early failures, followed by a stable phase and eventual wear-out failures, making the model suitable for reliability applications involving ageing mechanisms.

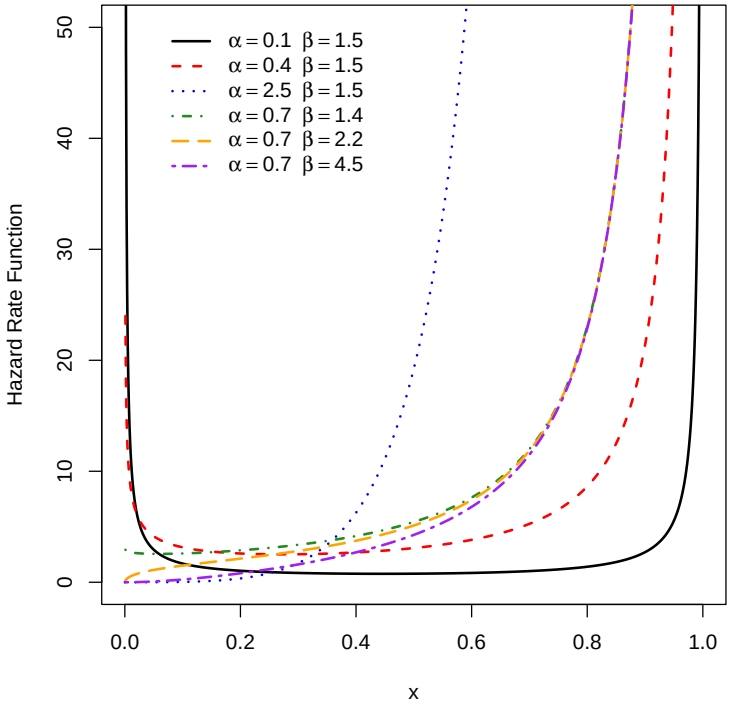

Figure 2. The HRF plots of TLRK distribution.

Note that the selection of parameter values for Figures 1 and 2 follows that standard practices in distributional modelling ([3, 32, 29]), the parameter configurations were systematically chosen to span the feasible positive quadrant $(\alpha, \beta) \in R^{+} \times R^{+}$ and capture all qualitatively distinct density and hazard regimes. This systematic coverage demonstrates the full flexibility of the TLRK distribution across its parameter space.

2.2. The CDF and PDF Expansion of TLRK Distribution

For practical purposes such as moment derivation and numerical computation, it is useful to express the CDF and PDF of the TLRK distribution as infinite series. These expansions rely on the binomial series and

the Taylor's series for the exponential function.

2.2.1. Expansion of the CDF

Recall the CDF from Equation (2.3):

$$F(x) = \left[1 - e^{-2\left(\frac{x}{1-x}\right)^{\alpha}}\right]^{\beta}, \quad x \in (0,1),\ \alpha,\beta > 0.$$

Apply the binomial expansion $(1-w)^{\beta} = \sum_{k=0}^{\infty} \binom{\beta}{k} (-1)^k w^k$, valid for with $|w| < 1$, Note that $0 < w < 1$ for all $x \in (0,1)$, so convergence is guaranteed. This gives:

$$F(x) = \sum_{k=0}^{\infty} \binom{\beta}{k} (-1)^k e^{-2k\left(\frac{x}{1-x}\right)^{\alpha}}.$$

expanding the exponential term using the Taylor's series $e^z = \sum_{m=0}^{\infty} \frac{z^m}{m!}$ with $z = -2k\left(\frac{x}{1-x}\right)^{\alpha}$:

$$e^{-2k\left(\frac{x}{1-x}\right)^{\alpha}} = \sum_{m=0}^{\infty} \frac{(-2k)^m}{m!} \left(\frac{x}{1-x}\right)^{m\alpha},$$

substituting back yields the complete series expansion for the CDF:

$$F(x) = \sum_{k=0}^{\infty} \sum_{m=0}^{\infty} \binom{\beta}{k} \frac{(-1)^k (-2k)^m}{m!} \left(\frac{x}{1-x}\right)^{m\alpha}. \tag{2.7}$$

2.2.2. Expansion of the PDF

Recall the PDF from Equation (2.4):

$$f(x) = 2\alpha\beta x^{\alpha-1}(1-x)^{-\alpha-1} e^{-2\left(\frac{x}{1-x}\right)^{\alpha}} \left[1 - e^{-2\left(\frac{x}{1-x}\right)^{\alpha}}\right]^{\beta-1}.$$

Apply the binomial expansion to the term $\left[1 - e^{-2\left(\frac{x}{1-x}\right)^{\alpha}}\right]^{\beta-1}$:

$$\left[1 - e^{-2\left(\frac{x}{1-x}\right)^{\alpha}}\right]^{\beta-1} = \sum_{k=0}^{\infty} \binom{\beta-1}{k} (-1)^k e^{-2k\left(\frac{x}{1-x}\right)^{\alpha}}.$$

Thus,

$$f(x) = 2\alpha\beta x^{\alpha-1}(1-x)^{-\alpha-1} \sum_{k=0}^{\infty} \binom{\beta-1}{k} (-1)^k e^{-2(k+1)\left(\frac{x}{1-x}\right)^{\alpha}},$$

expanding the remaining exponential factor using the Taylor series:

$$e^{-2(k+1)\left(\frac{x}{1-x}\right)^{\alpha}} = \sum_{m=0}^{\infty} \frac{(-2(k+1))^m}{m!} \left(\frac{x}{1-x}\right)^{m\alpha},$$

substituting gives the complete series expansion for the PDF:

$$f(x) = 2\alpha\beta x^{\alpha-1}(1-x)^{-\alpha-1}\sum_{k=0}^{\infty}\sum_{m=0}^{\infty}\binom{\beta-1}{k}\frac{(-1)^k(-2(k+1))^m}{m!}\left(\frac{x}{1-x}\right)^{m\alpha}. \tag{2.8}$$

Both expansions converge absolutely for all $x \in (0,1)$ because the binomial series converges when $\left|e^{-2(x/(1-x))^{\alpha}}\right| < 1$, which holds for all $x \in (0,1)$; and the Taylor's series for the exponential function converges for all finite arguments. However, these expansions are primarily useful for deriving theoretical properties such as moments and moment generating functions, as demonstrated in Sections 3.1 and 3.2.

3. Statistical Properties of TLRK Distribution

3.1. Moments

Moments are fundamental summary measures that describe the distributional characteristics of a random variable. The r-th moment about the origin provides information on location, dispersion, and higher-order shape features such as skewness and kurtosis. In particular, the first and second moments correspond to the mean and variance, respectively. Thus, the r-th moment of the TLRK distribution is derived as:

$$\mu'_r = E[X^r] = \int_0^1 x^r f(x)dx, \qquad r = 1,2,\ldots \tag{3.1}$$

substituting the PDF expansion from Equation (2.8) into (3.1) gives:

$$\mu'_r = 2\alpha\beta\sum_{k=0}^{\infty}\sum_{m=0}^{\infty}\binom{\beta-1}{k}\frac{(-1)^k(-2(k+1))^m}{m!}\int_0^1 x^{r+\alpha-1+m\alpha}(1-x)^{-\alpha-1}dx. \tag{3.2}$$

To evaluate the integral, apply the binomial series expansion to $(1-x)^{-\alpha-1}$:

$$(1-x)^{-\alpha-1} = \sum_{n=0}^{\infty}\binom{-\alpha-1}{n}(-1)^n x^n = \sum_{n=0}^{\infty}\binom{\alpha+n}{n}x^n,$$

where the identity $\binom{-\alpha-1}{n} = (-1)^n\binom{\alpha+n}{n}$ has been used. This series converges absolutely for $|x| < 1$, which holds on $(0,1)$; substituting this expansion into Equation (3.2) yields:

$$\mu'_r = 2\alpha\beta\sum_{k=0}^{\infty}\sum_{m=0}^{\infty}\sum_{n=0}^{\infty}\binom{\beta-1}{k}\binom{\alpha+n}{n}\frac{(-1)^k(-2(k+1))^m}{m!}\int_0^1 x^{r+\alpha-1+m\alpha+n}dx,$$

then the integral simplifies directly:

$$\int_0^1 x^{r+\alpha-1+m\alpha+n}dx = \frac{1}{r+\alpha+m\alpha+n}, \qquad r+\alpha+m\alpha+n > 0.$$

Thus, the r-th moment of the TLRK distribution is:

$$\mu'_r = 2\alpha\beta\sum_{k=0}^{\infty}\sum_{m=0}^{\infty}\sum_{n=0}^{\infty}\binom{\beta-1}{k}\binom{\alpha+n}{n}\frac{(-1)^k(-2(k+1))^m}{m!}\frac{1}{r+\alpha(1+m)+n}. \tag{3.3}$$

The first four moments are obtained by setting $r = 1, 2, 3, 4$ into Equation (3.3). The mean (μ), variance $\left(\sigma^2\right)$, coefficient of skewness (δ_1), and coefficient of kurtosis (δ_2) are then computed as:

$$\mu = \mu'_1,$$

$$\sigma^2 = \mu'_2 - (\mu'_1)^2,$$

$$\delta_1 = \frac{\mu'_3 - 3\mu'_2\mu'_1 + 2(\mu'_1)^3}{\sigma^3},$$

$$\delta_2 = \frac{\mu'_4 - 4\mu'_3\mu'_1 + 6\mu'_2(\mu'_1)^2 - 3(\mu'_1)^4}{\sigma^4}.$$

3.2. Moment Generating Function

The moment generating function (MGF) is a powerful tool that uniquely characterises a probability distribution. It is defined as $M_X(t) = E\left[e^{tX}\right]$, provided this expectation exists in a neighbourhood of zero. Additionally, the MGF facilitates the derivation of the distribution of sums of independent random variables and is widely used in convergence theorems.

The MGF of $X \sim TLRK(\alpha, \beta)$ is derived as:

$$M_X(t) = E[e^{tX}] = \int_0^1 e^{tx} f(x)dx, \qquad t \in \mathbb{R}.$$

Because X is bounded on $(0, 1)$, the MGF exists and is finite for all real t. Expanding the exponential function using its Taylor's series $e^{tx} = \sum_{p=0}^{\infty} \frac{t^p x^p}{p!}$ and interchanging summation and integration (justified by uniform convergence on $(0, 1)$) gives:

$$M_X(t) = \sum_{p=0}^{\infty} \frac{t^p}{p!} \int_0^1 x^p f(x)dx = \sum_{p=0}^{\infty} \mu'_p \frac{t^p}{p!} \tag{3.4}$$

Thus, the MGF is expressed directly as a power series whose coefficients are the moments derived in Section 3.1. Substituting the moment expression from Equation (3.3) into (3.4) yields the complete form:

$$M_X(t) = 2\alpha\beta \sum_{p=0}^{\infty}\sum_{k=0}^{\infty}\sum_{m=0}^{\infty}\sum_{n=0}^{\infty} \binom{\beta - 1}{k} \binom{\alpha + n}{n} \frac{(-1)^k(-2(k+1))^m}{m!\,p!} \frac{t^p}{p + \alpha(1+m) + n}. \tag{3.5}$$

Special case: When $\beta = 1$, the TLRK distribution reduces to the baseline RK distribution. Only the $k = 0$ term remains, giving:

$$M_X(t) = 2\alpha \sum_{p=0}^{\infty}\sum_{m=0}^{\infty}\sum_{n=0}^{\infty} \binom{\alpha + n}{n} \frac{(-2)^m}{m!\,p!} \frac{t^p}{p + \alpha(1+m) + n}. \tag{3.6}$$

3.3. Rényi Entropy

Rényi Entropy (RE) measures the uncertainty, disorder, or information content associated with a random variable. It quantifies the diversity or complexity of a distribution, with larger values indicating greater uncertainty. The RE is a generalisation of the Shannon entropy. Thus, the RE of order γ for a continuous random variable X with PDF $f(x)$ is defined as:

$$H_\gamma(X) = \frac{1}{1-\gamma}\log\left(\int_0^1 f^\gamma(x)dx\right), \qquad \gamma > 0,\ \gamma \neq 1. \tag{3.7}$$

As $\gamma \to 1, H_\gamma(X)$ converges to the Shannon entropy. The RE of the TLRK model is obtained as follows; from Equation (2.4):

$$f^\gamma(x) = (2\alpha\beta)^\gamma x^{\gamma(\alpha-1)}(1-x)^{-\gamma(\alpha+1)}e^{-2\gamma\left(\frac{x}{1-x}\right)^\alpha}\left[1-e^{-2\left(\frac{x}{1-x}\right)^\alpha}\right]^{\gamma(\beta-1)},$$

using the transformation $t = x/(1-x)$, the integral becomes:

$$\int_0^1 f^\gamma(x)dx = (2\alpha\beta)^\gamma \int_0^\infty t^{\gamma(\alpha-1)}(1+t)^{-\gamma(\alpha-1)-2}e^{-2\gamma t^\alpha}\left[1-e^{-2t^\alpha}\right]^{\gamma(\beta-1)}dt,$$

expanding the binomial term $\left[1-e^{-2t^\alpha}\right]^{\gamma(\beta-1)} = \sum_{k=0}^{\infty}\binom{\gamma(\beta-1)}{k}(-1)^k e^{-2kt^\alpha}$ yields:

$$\int_0^1 f^\gamma(x)dx = (2\alpha\beta)^\gamma \sum_{k=0}^{\infty}\binom{\gamma(\beta-1)}{k}(-1)^k \int_0^\infty t^{\gamma(\alpha-1)}(1+t)^{-\gamma(\alpha-1)-2}e^{-2(k+\gamma)t^\alpha}dt,$$

thus,

$$H_\gamma(X) = \frac{1}{1-\gamma}\log\left((2\alpha\beta)^\gamma \sum_{k=0}^{\infty}\binom{\gamma(\beta-1)}{k}(-1)^k \int_0^\infty t^{\gamma(\alpha-1)}(1+t)^{-\gamma(\alpha-1)-2}e^{-2(k+\gamma)t^\alpha}dt.\right), \tag{3.8}$$

For general γ, Equation (3.8) requires numerical evaluation. The special case $\gamma = 2$ can be expressed using gamma functions and the confluent hypergeometric function, but for most practical purposes, direct numerical integration of $\int_0^1 f^\gamma(x)dx$ is recommended. The Shannon entropy ($\gamma = 1$) is obtained by numerical integration of $-f(x)\log f(x)$.

3.4. Quantile Function

The quantile function is the inverse of the cumulative distribution function, denoted $Q(p) = F^{-1}(p)$ for $p \in (0,1)$. It specifies the value below which a given proportion p of the distribution lies. Quantiles are essential for generating random samples from a distribution via the inverse transform method, constructing confidence intervals, and computing robust summary statistics such as the median, interquartile range, and other percentile-based measures. Unlike moments, quantiles are less sensitive to outliers and can characterise distributions that lack finite moments.

For the TLRK distribution, the quantile function is obtained by inverting the CDF given in Equation (2.3), which yields:

$$Q(p) = \frac{1}{1 + \left[-\frac{1}{2}\log\left(1 - p^{1/\beta}\right)\right]^{-1/\alpha}}, \quad p \in (0,1), \tag{3.9}$$

Note that the median, lower and upper interquartile ranges of the TLRK model are respectively obtained by inserting $p = 0.5$, $p = 0.25$ and $p = 0.75$ into Equation (3.9). Thus, its median is given by:

$$Q_2 = \frac{1}{1 + \left[-\frac{1}{2}\log\left(1 - 0.5^{1/\beta}\right)\right]^{-1/\alpha}}. \tag{3.10}$$

A random sample can be generated from Equation (3.9) by treating p as a uniformly distributed random variable.

3.5. Skewness and Kurtosis

Bowley's skewness (based on quartiles) by [23] and Moors' kurtosis (based on octiles) by [27] are robust measures of asymmetry and tail weight, respectively, that do not rely on moments. The Bowley's skewness (BS) and Moors' kurtosis (MK) for the TLRK distribution can be derived from Equation (3.9), with their respective definitions given as follows:

$$BS = \frac{Q_3 - 2Q_2 + Q_1}{Q_3 - Q_1} \tag{3.11}$$

and

$$MK = \frac{O_7 - O_5 + O_3 - O_1}{Q_3 - Q_1}, \tag{3.12}$$

where Q_i and O_j are the i-th quartile and j-th octile of the TLRK distribution, that is, $Q_i = Q(i/4)$, $i = 1, 2, 3$ and $O_j = Q(j/8)$, $j = 1, 3, 5, 7$. The BS can either take negative values which indicate left skewness, positive values which indicate right skewness, or zero which indicates symmetry. On the other hand, MK describes the peakedness and tail heaviness, with larger values indicating heavier tails. These measures are particularly useful for distributions such as the TLRK model, where moments may be difficult to interpret due to bounded support.

Figure 3 displays these measures across a range of parameter values. From the plots, it is observed that the Bowley's skewness may assume either negative or positive values, reflecting left- or right-skewed characteristics of the TLRK distribution. Furthermore, the kurtosis exhibits a non-monotonic behaviour, with values spanning a wide range from low to high magnitudes.

4. Estimation Methods

Here, seven estimators are examined for the estimation of the parameters of TLRK distribution.

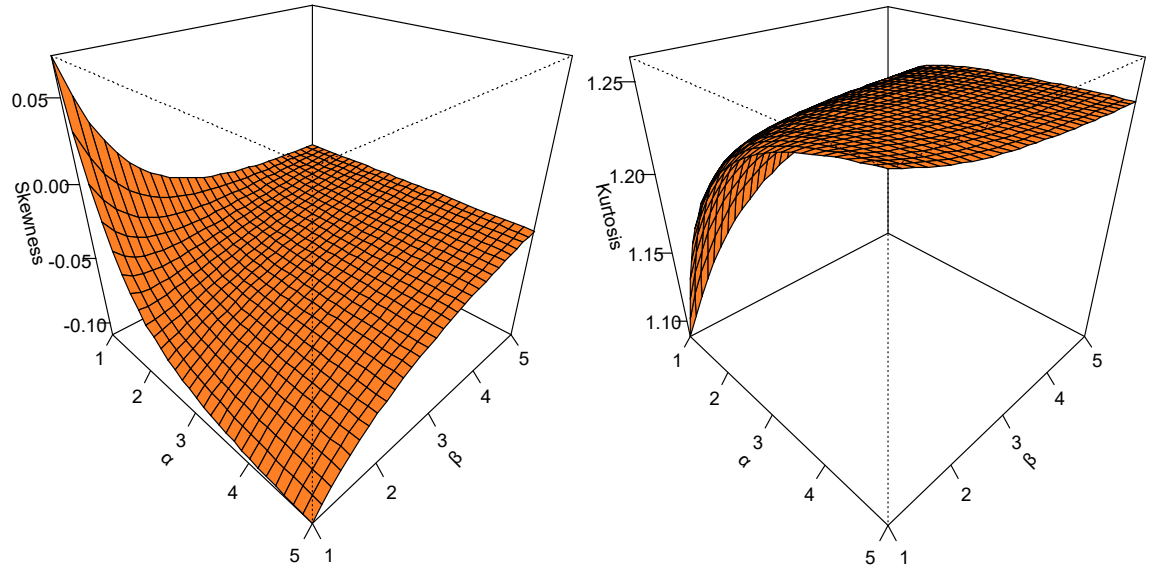

Figure 3. The Bowley's skewness and Moors' kurtosis plots of TLRK distribution.

4.1. Maximum Likelihood Estimator (MLE)

The method of maximum likelihood estimates (MLEs) model parameters by maximising the log-likelihood function derived from the joint density of the observed sample. Under standard regularity conditions, the estimators are consistent, asymptotically normal and efficient, forming the theoretical foundation of modern parametric inference [17]. Let $x_1, x_2, ..., x_n$ be a random sample from the TLRK distribution; then, the log-likelihood function is given by:

$$\begin{aligned}\ell(\alpha,\beta) &= n\ln(2) + n\ln(\alpha) + n\ln(\beta) + (\alpha-1)\sum_{i=1}^{n}\ln(x_i) - (\alpha+1)\sum_{i=1}^{n}\ln(1-x_i) \\ &\quad - 2\sum_{i=1}^{n}\left(\frac{x_i}{1-x_i}\right) + (\beta-1)\sum_{i=1}^{n}\ln\left(1-e^{-2\left(\frac{x_i}{1-x_i}\right)^{\alpha}}\right)\end{aligned} \tag{4.1}$$

Taking partial derivatives of ℓ with respect to α and β and set them to zero, the MLEs of α and β are obtained as:

$$\begin{aligned}\frac{\partial\ell}{\partial\alpha} &= \frac{n}{\alpha} + \sum_{i=1}^{n}\ln(x_i) - \sum_{i=1}^{n}\ln(1-x_i) - 2\sum_{i=1}^{n}\left(\frac{x_i}{1-x_i}\right)^{\alpha}\ln\left(\frac{x_i}{1-x_i}\right) \\ &\quad + (\beta-1)\sum_{i=1}^{n}\ln\left(\frac{2\left(\frac{x_i}{1-x_i}\right)^{\alpha}\ln\left(\frac{x_i}{1-x_i}\right)e^{-2\left(\frac{x_i}{1-x_i}\right)^{\alpha}}}{1-e^{-2\left(\frac{x_i}{1-x_i}\right)^{\alpha}}}\right) = 0,\end{aligned} \tag{4.2}$$

$$\frac{\partial\ell}{\partial\beta} = \frac{n}{\beta} + \sum_{i=1}^{n}\ln\left(1-e^{-2\left(\frac{x_i}{1-x_i}\right)^{\alpha}}\right) = 0. \tag{4.3}$$

This system of equations is non-linear and typically requires numerical methods to solve via the aid of R software.

4.2. Least Square Estimator (LSE)

The least squares method minimises the squared differences between fitted cumulative probabilities and their expected plotting positions. It offers computational simplicity and reasonable efficiency in distributional estimation [34]. The least squares estimates, $\hat{\alpha}_{LSE}$ and $\hat{\beta}_{LSE}$, of α and β respectively, are derived by minimising:

$$S(\alpha,\beta) = \sum_{i=1}^{n}\left[\left(1 - e^{-2\left(\frac{x_{(i)}}{1-x_{(i)}}\right)^{\alpha}}\right)^{\beta} - \frac{i}{n+1}\right]^2 \tag{4.4}$$

4.3. Cramér-von Mises Estimator (CVME)

The Cramér-von Mises (CVM) method estimates parameters by minimising the integrated squared deviation between empirical and fitted distribution functions. It applies uniform weighting across the support, yielding stable and consistent estimators [11]. The CVM estimates, $\hat{\alpha}_{CVM}$ and $\hat{\beta}_{CVM}$, of α and β respectively, are obtained by minimising:

$$C(\alpha,\beta) = \frac{1}{12n} + \sum_{i=1}^{n}\left[\left(1 - e^{-2\left(\frac{x_{(i)}}{1-x_{(i)}}\right)^{\alpha}}\right)^{\beta} - \frac{2i-1}{2n}\right]^2. \tag{4.5}$$

4.4. Maximum Product of Spacings Estimator (MPSE)

The maximum product of spacings (MPS) method maximises the geometric mean of the cumulative probability spacings between ordered observations. It provides robust and asymptotically efficient estimation, particularly when the likelihood function is numerically unstable [21]. The MPS estimates, $\hat{\alpha}_{MPS}$ and $\hat{\beta}_{MPS}$, of α and β are respectively obtained by maximising:

$$M(\alpha,\beta) = \frac{1}{n+1} + \sum_{i=1}^{n+1}\log\left[\left(1 - e^{-2\left(\frac{x_{(i)}}{1-x_{(i)}}\right)^{\alpha}}\right)^{\beta} - \left(1 - e^{-2\left(\frac{x_{(i-1)}}{1-x_{(i-1)}}\right)^{\alpha}}\right)^{\beta}\right]^2. \tag{4.6}$$

4.5. Anderson Darling Estimator (ADE)

The Anderson-Darling method minimises a weighted squared distance between the empirical and theoretical distribution functions, assigning greater weight to tail observations. Its asymptotic properties and tail sensitivity make it a powerful goodness-of-fit and estimation tool in distributional modelling [6]. The Anderson-Darling estimates, $\hat{\alpha}_{ADE}$ and $\hat{\beta}_{ADE}$, of α and β are respectively obtained by minimising:

$$A(\alpha,\beta) = -n - \frac{1}{n}\sum_{i=1}^{n}(2i-1)\left[\log\left(1 - e^{-2\left(\frac{x_{(i)}}{1-x_{(i)}}\right)^{\alpha}}\right)^{\beta} + \log\left(1 - e^{-2\left(\frac{x_{(i)}}{1-x_{(i)}}\right)^{\alpha}}\right)^{\beta}\right]^2. \tag{4.7}$$

4.6. Weighted Least Squares Estimator (WLSE)

Weighted least squares (WLS) incorporates variance-based weights into the least squares criterion to account for heteroscedasticity in order statistics. This improves estimation efficiency relative to ordinary least squares [34]. The WLS estimates, $\hat{\alpha}_{WLS}$ and $\hat{\beta}_{WLS}$, of α and β respectively, are derived by minimising:

$$W(\alpha,\beta) = \sum_{i=1}^{n}\frac{(n+1)^2(n+2)}{i(n-i+1)}\sum_{i=1}^{n}\left[\left(1 - e^{-2\left(\frac{x_{(i)}}{1-x_{(i)}}\right)^{\alpha}}\right)^{\beta} - \frac{i}{n+1}\right]^2. \tag{4.8}$$

4.7. *Percentile-Based Estimator (PBE)*

The percentile-based method estimates parameters by minimising the squared difference between observed order statistics and theoretical quantiles. It is especially useful in reliability and lifetime modelling where quantile interpretation is central [22]. The Percentile-Based estimates, $\hat{\alpha}_{PBE}$ and $\hat{\beta}_{PBE}$, of α and β respectively, are derived by minimising:

$$P(\alpha,\beta) = \sum_{i=1}^{n}\left[\frac{1}{1+\left(-0.5\log\left(1-{p_i}^{1/\beta}\right)\right)^{-1/\alpha}} - \hat{q}_{p_i}\right]^2, \tag{4.9}$$

where $\hat{q}(p_i)$ is the empirical (sample) percentile at $p_1, p_2, ..., p_k$ selected probabilities.

Equations (4.4) - (4.9) involve non-linear functions, hence, require numerical optimisation techniques to minimise or maximise the respective objective functions.

5. Simulation

A Monte Carlo simulation study was conducted to evaluate the performance of seven estimators for the TLRK distribution under varying simulation conditions. The simulations were implemented using the R software. Random samples of sizes $n = 20, 40, \ldots, 200$ were generated from the TLRK distribution, with each experiment replicated 1000 times to ensure robustness. The assessment was based on two key metrics: estimated bias and mean squared error (MSE). The parameter combinations $(\alpha = 0.8, \beta = 1.5)$, $(\alpha = 2.5, \beta = 1.2)$, $(\alpha = 1.4, \beta = 2.7)$, and $(\alpha = 3.7, \beta = 3.3)$ were examined. The bias and MSE are computed by:

$$Bias = \frac{1}{1000}\sum_{i=1}^{1000}(\hat{\omega}_i - \omega), \quad MSE = \frac{1}{1000}\sum_{i=1}^{1000}(\hat{\omega}_i - \omega)^2,$$

respectively, where $\omega = \alpha$ or β.

The outcomes of these simulations are presented in Tables 1 - 4, together with their graphical representations illustrated in Figures 4 - 7. The following were observed:

1. MSE generally decreases with increasing sample size for all estimators, confirming consistency, though minor non-monotone fluctuations are occasionally observed at intermediate sample sizes.
2. MPSE attains the lowest MSE most frequently, particularly for the shape parameter α, across all four parameter settings; MLE is a close and consistent competitor, especially for β. ADE also performs competitively, yielding the lowest α-MSE in several scenarios of Table 1. CVME and WLSE exhibit moderate performance, whilst LSE and PBE are generally least efficient.
3. MPSE and ADE are more stable for small n, often yielding lower variability than MLE. CVM and WLSE are moderately stable; LSE and PBE show higher dispersion.
4. Best for β: MLE is best for β in Table 1 across all sample sizes; MPSE is best or joint-best for β in Tables 2 - 4. β is generally underestimated by most estimators; only MLE and MPSE exhibit a consistent positive bias for β. LSE and WLSE most consistently underestimate β.
5. Best for α: MPSE consistently yields the lowest α-MSE across Tables 2 - 4, with MLE as a close competitor; in Table 1, ADE attains the lowest α-MSE at most sample sizes. α is consistently overestimated across all methods and parameter configurations; PBE generally yields the highest α-MSE, though LSE is worst at small sample sizes under large α values (Table 2).

6. Bias and MSE increase under more extreme parameter values, indicating sensitivity to distributional shape across all methods.

Furthermore, Figures 4 - 7 provide visual confirmation. In all four Figures:

1. The bias plots show that the MLE, MPSE and ADE converge to zero bias fastest, while PBE for α shows persistent positive bias even at $n = 200$.
2. The MSE plots show that MLE and MPSE are nearly overlapping for $n \geqslant 80$, with ADE slightly above.
3. LSE and WLSE show consistently higher MSE, with LSE performing particularly poorly for β estimation.
4. The rate of decrease in MSE is steepest between $n = 20$ and $n = 60$, flattening thereafter.

Therefore, MPSE and MLE converge fastest with tighter dispersion, followed closely by ADE; CVME and WLSE show moderate convergence; LSE and PBE converge more slowly with wider spread.

Table 1. The bias and MSE of different methods of estimations of the TLRK distribution at $(\alpha = 0.8, \beta = 1.5)$.

n		ADE$(\hat{\alpha},\hat{\beta})$	CVME$(\hat{\alpha},\hat{\beta})$	LSE$(\hat{\alpha},\hat{\beta})$	MLE$(\hat{\alpha},\hat{\beta})$	MPSE$(\hat{\alpha},\hat{\beta})$	PBE$(\hat{\alpha},\hat{\beta})$	WLSE$(\hat{\alpha},\hat{\beta})$
20	Bias	(0.225, -0.057)	(0.277, -0.040)	(0.414, -0.049)	(0.345, 0.044)	(0.148, 0.191)	(0.418, -0.013)	(0.278, -0.121)
	MSE	(0.563, 0.328)	(0.907, 0.452)	(1.050, 0.093)	(0.620, 0.075)	(0.498, 0.147)	(1.850, 0.581)	(0.438, 0.395)
40	Bias	(0.075, -0.036)	(0.093, -0.022)	(0.290, -0.026)	(0.185, 0.025)	(0.090, 0.107)	(0.227, -0.021)	(0.126, -0.053)
	MSE	(0.055, 0.166)	(0.107, 0.244)	(0.641, 0.074)	(0.233, 0.038)	(0.253, 0.062)	(0.923, 0.348)	(0.105, 0.205)
60	Bias	(0.050, -0.023)	(0.072, -0.023)	(0.236, -0.027)	(0.127, 0.023)	(0.025, 0.092)	(0.171, -0.025)	(0.087, -0.056)
	MSE	(0.027, 0.107)	(0.059, 0.170)	(0.450, 0.054)	(0.138, 0.026)	(0.097, 0.038)	(0.531, 0.255)	(0.048, 0.140)
80	Bias	(0.035, -0.025)	(0.054, -0.026)	(0.186, -0.021)	(0.088, 0.024)	(0.012, 0.083)	(0.137, -0.035)	(0.065, -0.046)
	MSE	(0.017, 0.071)	(0.045, 0.120)	(0.337, 0.045)	(0.078, 0.021)	(0.063, 0.032)	(0.475, 0.191)	(0.031, 0.104)
100	Bias	(0.028, -0.008)	(0.045, -0.007)	(0.173, -0.015)	(0.073, 0.019)	(0.008, 0.067)	(0.075, -0.004)	(0.057, -0.053)
	MSE	(0.014, 0.060)	(0.088, 0.103)	(0.330, 0.040)	(0.049, 0.017)	(0.041, 0.024)	(0.186, 0.154)	(0.023, 0.081)
120	Bias	(0.021, -0.008)	(0.030, -0.012)	(0.150, -0.015)	(0.059, 0.020)	(-0.006, 0.065)	(0.053, -0.012)	(0.040, -0.029)
	MSE	(0.010, 0.053)	(0.021, 0.085)	(0.261, 0.036)	(0.035, 0.014)	(0.024, 0.019)	(0.084, 0.121)	(0.014, 0.062)
140	Bias	(0.021, -0.015)	(0.026, -0.012)	(0.129, -0.015)	(0.056, 0.016)	(0.005, 0.053)	(0.045, -0.008)	(0.031, -0.026)
	MSE	(0.009, 0.044)	(0.016, 0.069)	(0.223, 0.030)	(0.037, 0.013)	(0.026, 0.017)	(0.105, 0.104)	(0.012, 0.052)
160	Bias	(0.015, -0.009)	(0.025, -0.012)	(0.102, -0.008)	(0.048, 0.016)	(0.000, 0.051)	(0.038, -0.013)	(0.032, -0.024)
	MSE	(0.007, 0.038)	(0.016, 0.069)	(0.180, 0.028)	(0.027, 0.011)	(0.020, 0.015)	(0.035, 0.102)	(0.011, 0.052)
180	Bias	(0.013, -0.008)	(0.019, -0.009)	(0.076, -0.007)	(0.045, 0.013)	(-0.001, 0.048)	(0.033, -0.008)	(0.027, -0.017)
	MSE	(0.006, 0.032)	(0.013, 0.054)	(0.114, 0.023)	(0.024, 0.009)	(0.020, 0.013)	(0.042, 0.085)	(0.009, 0.041)
200	Bias	(0.009, 0.002)	(0.011, 0.003)	(0.060, -0.001)	(0.036, 0.016)	(-0.006, 0.047)	(0.016, 0.009)	(0.029, -0.026)
	MSE	(0.005, 0.027)	(0.009, 0.045)	(0.090, 0.020)	(0.019, 0.008)	(0.014, 0.011)	(0.021, 0.067)	(0.008, 0.038)

6. Applications

This study evaluates the flexibility of the TLRK distribution by analyzing two real datasets and comparing its performance against established competing models. The competing models include: the Extended Reduced Kies (ExRK), the Exponential Reduced Kies (ERK), Marshall-Olkin Reduced Kies (MORK), and Reduced Kies (RK). The PDF of these fitted models (for all $\alpha > 0, \beta > 0, 0 < x < 1$) are given as follows:

- ExRK by [5]: $f(x;\alpha,\beta) = \dfrac{\alpha\beta(x/(1-x))^{\alpha-1}\left(1-e^{-(x/(1-x))^{\alpha}}\right)^{\beta}}{(x-1)^2\ln(2)\left[e^{(x/(1-x))^{\alpha}}-1\right]\left(\left(1-e^{-(x/(1-x))^{\alpha}}\right)^{\beta}+1\right)}$,
- ERK by [26]: $f(x;\alpha,\beta) = \beta\alpha x^{\alpha-1}(1-x)^{-\alpha-1}e^{-(x/(1-x))^{\beta}}\left(1-e^{-(x/(1-x))^{\beta}}\right)^{\alpha-1}$,

Table 2. The bias and MSE of different methods of estimations of the TLRK distribution at $(\alpha = 2.5, \beta = 1.2)$.

n		ADE$(\hat{\alpha},\hat{\beta})$	CVME$(\hat{\alpha},\hat{\beta})$	LSE$(\hat{\alpha},\hat{\beta})$	MLE$(\hat{\alpha},\hat{\beta})$	MPSE$(\hat{\alpha},\hat{\beta})$	PBE$(\hat{\alpha},\hat{\beta})$	WLSE$(\hat{\alpha},\hat{\beta})$
20	Bias	(0.902, -0.059)	(0.884, 0.001)	(1.397, -0.182)	(0.690, -0.046)	(0.002, 0.151)	(0.857, 0.050)	(0.896, -0.080)
	MSE	(7.040, 0.255)	(9.739, 0.362)	(14.704, 0.347)	(3.676, 0.239)	(2.475, 0.273)	(5.912, 0.473)	(4.291, 0.310)
40	Bias	(0.292, -0.003)	(0.446, 0.020)	(0.601, -0.077)	(0.321, -0.039)	(-0.074, 0.082)	(0.636, 0.025)	(0.453, -0.055)
	MSE	(1.138, 0.132)	(4.090, 0.222)	(4.104, 0.214)	(1.007, 0.116)	(0.486, 0.123)	(3.981, 0.312)	(1.259, 0.155)
60	Bias	(0.151, -0.004)	(0.238, 0.009)	(0.329, -0.056)	(0.147, -0.011)	(-0.112, 0.078)	(0.466, 0.010)	(0.337, -0.060)
	MSE	(0.320, 0.076)	(1.618, 0.134)	(1.669, 0.133)	(0.334, 0.072)	(0.229, 0.079)	(2.648, 0.221)	(0.822, 0.109)
80	Bias	(0.132, -0.013)	(0.204, -0.015)	(0.274, -0.064)	(0.121, -0.015)	(-0.089, 0.057)	(0.480, -0.031)	(0.229, -0.039)
	MSE	(0.246, 0.062)	(0.555, 0.105)	(0.667, 0.106)	(0.235, 0.057)	(0.176, 0.061)	(2.458, 0.177)	(0.396, 0.083)
100	Bias	(0.093, -0.011)	(0.145, -0.006)	(0.197, -0.045)	(0.087, -0.011)	(-0.086, 0.050)	(0.366, -0.019)	(0.181, -0.027)
	MSE	(0.167, 0.048)	(0.415, 0.091)	(0.475, 0.092)	(0.156, 0.045)	(0.128, 0.048)	(1.816, 0.153)	(0.278, 0.063)
120	Bias	(0.072, -0.002)	(0.103, 0.004)	(0.143, -0.028)	(0.085, -0.014)	(-0.066, 0.039)	(0.277, -0.004)	(0.176, -0.042)
	MSE	(0.122, 0.038)	(0.276, 0.070)	(0.309, 0.070)	(0.137, 0.040)	(0.114, 0.041)	(1.313, 0.124)	(0.216, 0.053)
140	Bias	(0.065, -0.006)	(0.078, 0.005)	(0.111, -0.024)	(0.076, -0.014)	(-0.059, 0.033)	(0.180, 0.007)	(0.157, -0.040)
	MSE	(0.100, 0.032)	(0.204, 0.057)	(0.225, 0.057)	(0.110, 0.033)	(0.091, 0.034)	(0.873, 0.101)	(0.185, 0.045)
160	Bias	(0.062, -0.010)	(0.090, -0.003)	(0.119, -0.028)	(0.061, -0.009)	(-0.060, 0.034)	(0.193, -0.011)	(0.109, -0.019)
	MSE	(0.086, 0.028)	(0.206, 0.055)	(0.224, 0.055)	(0.094, 0.030)	(0.080, 0.031)	(0.709, 0.092)	(0.146, 0.040)
180	Bias	(0.051, -0.010)	(0.070, -0.008)	(0.095, -0.030)	(0.052, -0.008)	(-0.058, 0.031)	(0.140, -0.009)	(0.089, -0.013)
	MSE	(0.077, 0.026)	(0.161, 0.044)	(0.174, 0.045)	(0.081, 0.025)	(0.071, 0.026)	(0.569, 0.074)	(0.114, 0.035)
200	Bias	(0.055, -0.007)	(0.071, -0.002)	(0.094, -0.022)	(0.050, -0.008)	(-0.052, 0.029)	(0.161, -0.011)	(0.100, -0.020)
	MSE	(0.067, 0.024)	(0.148, 0.043)	(0.158, 0.043)	(0.072, 0.024)	(0.063, 0.025)	(0.530, 0.077)	(0.115, 0.034)

Table 3. The bias and MSE of different methods of estimations of the TLRK distribution at $(\alpha = 1.4, \beta = 2.7)$.

n		ADE$(\hat{\alpha},\hat{\beta})$	CVME$(\hat{\alpha},\hat{\beta})$	LSE$(\hat{\alpha},\hat{\beta})$	MLE$(\hat{\alpha},\hat{\beta})$	MPSE$(\hat{\alpha},\hat{\beta})$	PBE$(\hat{\alpha},\hat{\beta})$	WLSE$(\hat{\alpha},\hat{\beta})$
20	Bias	(0.205, -0.042)	(0.279, -0.049)	(0.395, -0.332)	(0.151, 0.017)	(-0.082, 0.155)	(0.331, -0.038)	(0.279, -0.011)
	MSE	(0.373, 0.715)	(0.828, 0.945)	(1.272, 0.942)	(0.208, 0.701)	(0.139, 0.645)	(1.391, 1.020)	(0.444, 0.890)
40	Bias	(0.072, 0.017)	(0.079, 0.043)	(0.113, -0.102)	(0.077, -0.014)	(-0.062, 0.077)	(0.103, 0.052)	(0.145, -0.046)
	MSE	(0.062, 0.317)	(0.124, 0.431)	(0.144, 0.415)	(0.068, 0.299)	(0.051, 0.283)	(0.360, 0.503)	(0.125, 0.391)
60	Bias	(0.054, 0.004)	(0.065, -0.002)	(0.087, -0.098)	(0.039, 0.008)	(-0.062, 0.076)	(0.072, 0.002)	(0.097, -0.041)
	MSE	(0.040, 0.211)	(0.066, 0.270)	(0.073, 0.269)	(0.034, 0.195)	(0.031, 0.190)	(0.109, 0.313)	(0.138, 0.270)
80	Bias	(0.043, -0.014)	(0.059, -0.028)	(0.074, -0.100)	(0.030, -0.001)	(-0.051, 0.055)	(0.058, -0.020)	(0.067, -0.032)
	MSE	(0.028, 0.154)	(0.047, 0.203)	(0.051, 0.207)	(0.026, 0.146)	(0.024, 0.142)	(0.081, 0.233)	(0.041, 0.188)
100	Bias	(0.038, -0.020)	(0.041, -0.015)	(0.053, -0.073)	(0.023, -0.003)	(-0.045, 0.044)	(0.039, -0.006)	(0.053, -0.025)
	MSE	(0.022, 0.123)	(0.034, 0.151)	(0.036, 0.153)	(0.019, 0.118)	(0.019, 0.115)	(0.053, 0.171)	(0.032, 0.143)
120	Bias	(0.027, -0.007)	(0.031, -0.005)	(0.041, -0.053)	(0.024, -0.008)	(-0.035, 0.034)	(0.034, -0.003)	(0.053, -0.018)
	MSE	(0.017, 0.106)	(0.028, 0.133)	(0.029, 0.134)	(0.018, 0.102)	(0.016, 0.100)	(0.046, 0.154)	(0.027, 0.119)
140	Bias	(0.023, -0.012)	(0.026, -0.008)	(0.034, -0.049)	(0.021, -0.008)	(-0.031, 0.029)	(0.030, -0.007)	(0.040, -0.018)
	MSE	(0.015, 0.091)	(0.024, 0.125)	(0.025, 0.125)	(0.014, 0.084)	(0.014, 0.082)	(0.043, 0.147)	(0.019, 0.106)
160	Bias	(0.014, 0.004)	(0.009, 0.015)	(0.017, -0.021)	(0.016, -0.003)	(-0.030, 0.030)	(0.004, 0.021)	(0.035, -0.006)
	MSE	(0.012, 0.076)	(0.020, 0.100)	(0.020, 0.099)	(0.013, 0.075)	(0.012, 0.074)	(0.031, 0.111)	(0.016, 0.088)
180	Bias	(0.017, -0.003)	(0.020, -0.009)	(0.027, -0.041)	(0.014, -0.004)	(-0.029, 0.026)	(0.019, -0.003)	(0.041, -0.034)
	MSE	(0.010, 0.069)	(0.017, 0.091)	(0.018, 0.091)	(0.011, 0.062)	(0.011, 0.061)	(0.029, 0.109)	(0.016, 0.087)
200	Bias	(0.014, 0.000)	(0.021, -0.005)	(0.027, -0.034)	(0.014, -0.002)	(-0.026, 0.025)	(0.027, -0.009)	(0.027, -0.004)
	MSE	(0.009, 0.062)	(0.015, 0.084)	(0.016, 0.084)	(0.010, 0.061)	(0.010, 0.060)	(0.028, 0.101)	(0.013, 0.072)

- MORK by [2]: $f(x;\alpha,\beta) = \frac{\alpha\beta x^{\alpha-1}(1-x)^{-\alpha-1}e^{-(x/(1-x))^{\alpha}}}{\left(1-(1-\beta)e^{-(x/(1-x))^{\alpha}}\right)^2}$,
- RK by [25]: $f(x;\alpha) = \alpha x^{\alpha-1}(1-x)^{-\alpha-1}e^{-(x/(1-x))^{\alpha}}$.

The most suitable distribution for each dataset was selected based on the following goodness-of-fit statistics: the log-likelihood (ℓ), Akaike Information Criterion (AIC), Bayesian Information Criterion (BIC), Consistent Akaike Information Criterion (CAIC), Hannan-Quinn Information Criterion (HQIC), Cramér-

Table 4. The bias and MSE of different methods of estimations of the TLRK distribution at $(\alpha = 3.7, \beta = 3.3)$.

n		ADE$(\hat{\alpha},\hat{\beta})$	CVME$(\hat{\alpha},\hat{\beta})$	LSE$(\hat{\alpha},\hat{\beta})$	MLE$(\hat{\alpha},\hat{\beta})$	MPSE$(\hat{\alpha},\hat{\beta})$	PBE$(\hat{\alpha},\hat{\beta})$	WLSE$(\hat{\alpha},\hat{\beta})$
20	Bias	(0.402, 0.004)	(0.450, 0.013)	(0.653, -0.312)	(0.363, 0.040)	(-0.226, 0.136)	(0.396, 0.019)	(0.672, 0.038)
	MSE	(1.465, 0.907)	(1.950, 1.070)	(2.716, 1.049)	(1.184, 0.971)	(0.720, 0.824)	(2.486, 1.099)	(2.085, 1.184)
40	Bias	(0.141, 0.018)	(0.169, 0.027)	(0.244, -0.136)	(0.177, -0.001)	(-0.164, 0.064)	(0.163, 0.031)	(0.317, -0.028)
	MSE	(0.345, 0.427)	(0.570, 0.559)	(0.643, 0.544)	(0.379, 0.393)	(0.302, 0.359)	(0.918, 0.614)	(0.648, 0.473)
60	Bias	(0.099, 0.009)	(0.114, 0.001)	(0.162, -0.108)	(0.087, 0.018)	(-0.159, 0.066)	(0.090, 0.007)	(0.214, 0.019)
	MSE	(0.205, 0.272)	(0.351, 0.330)	(0.381, 0.329)	(0.196, 0.257)	(0.184, 0.243)	(0.519, 0.354)	(0.332, 0.336)
80	Bias	(0.091, -0.015)	(0.097, -0.013)	(0.132, -0.094)	(0.067, 0.006)	(-0.131, 0.046)	(0.088, -0.003)	(0.161, -0.015)
	MSE	(0.163, 0.191)	(0.254, 0.246)	(0.270, 0.248)	(0.148, 0.189)	(0.143, 0.181)	(0.414, 0.272)	(0.223, 0.255)
100	Bias	(0.065, -0.007)	(0.064, -0.008)	(0.092, -0.073)	(0.051, 0.001)	(-0.115, 0.035)	(0.060, -0.006)	(0.120, -0.008)
	MSE	(0.116, 0.155)	(0.191, 0.195)	(0.200, 0.196)	(0.112, 0.153)	(0.111, 0.147)	(0.324, 0.217)	(0.167, 0.184)
120	Bias	(0.043, 0.022)	(0.057, 0.019)	(0.079, -0.035)	(0.054, -0.003)	(-0.091, 0.026)	(0.063, 0.013)	(0.120, -0.025)
	MSE	(0.102, 0.132)	(0.166, 0.169)	(0.173, 0.167)	(0.102, 0.132)	(0.098, 0.127)	(0.269, 0.187)	(0.138, 0.157)
140	Bias	(0.052, 0.006)	(0.059, 0.003)	(0.078, -0.044)	(0.048, -0.004)	(-0.080, 0.022)	(0.060, -0.001)	(0.083, -0.016)
	MSE	(0.079, 0.117)	(0.133, 0.154)	(0.138, 0.154)	(0.084, 0.108)	(0.081, 0.105)	(0.220, 0.167)	(0.100, 0.122)
160	Bias	(0.026, 0.021)	(0.027, 0.027)	(0.043, -0.014)	(0.037, 0.001)	(-0.078, 0.024)	(0.029, 0.023)	(0.083, -0.013)
	MSE	(0.071, 0.101)	(0.112, 0.123)	(0.114, 0.120)	(0.073, 0.096)	(0.072, 0.094)	(0.190, 0.139)	(0.090, 0.109)
180	Bias	(0.037, 0.010)	(0.041, 0.016)	(0.056, -0.020)	(0.031, -0.001)	(-0.073, 0.021)	(0.045, 0.015)	(0.066, -0.007)
	MSE	(0.065, 0.086)	(0.103, 0.109)	(0.106, 0.108)	(0.064, 0.080)	(0.064, 0.078)	(0.175, 0.120)	(0.083, 0.100)
200	Bias	(0.029, -0.005)	(0.039, -0.011)	(0.052, -0.044)	(0.031, 0.000)	(-0.066, 0.021)	(0.045, -0.010)	(0.075, -0.012)
	MSE	(0.053, 0.078)	(0.088, 0.100)	(0.090, 0.100)	(0.061, 0.078)	(0.060, 0.077)	(0.160, 0.115)	(0.080, 0.093)

von Mises (W*), Anderson-Darling (A*), and Kolmogorov-Smirnov (KS) and its associated p-value. Two datasets were selected to represent differing distributional characteristics, including positive and negative skewness, thereby enabling a robust assessment of the model across varying data structures.

Dataset I: Failure Times of Kevlar 49/Epoxy Strands: This dataset comprises 58 observations of failure times for Kevlar 49/epoxy strands tested at 90% stress level [31]. The data points are: 0.01, 0.01, 0.02, 0.02, 0.02, 0.03, 0.03, 0.04, 0.05, 0.06, 0.07, 0.07, 0.08, 0.09, 0.09, 0.10, 0.10, 0.11, 0.11, 0.12, 0.13, 0.18, 0.19, 0.20, 0.23, 0.24, 0.24, 0.29, 0.34, 0.35, 0.36, 0.38, 0.40, 0.42, 0.43, 0.52, 0.54, 0.56, 0.60, 0.60, 0.63, 0.65, 0.67, 0.68, 0.72, 0.72, 0.72, 0.73, 0.79, 0.79, 0.80, 0.80, 0.83, 0.85, 0.90, 0.92, 0.95, 0.99.

Dataset II: Relief Times of Arthritic Patients: This dataset records relief times (in hours) for 50 arthritic patients, as originally published by [38]. The measurements are: 0.70, 0.84, 0.58, 0.50, 0.55, 0.82, 0.59, 0.71, 0.72, 0.61, 0.62, 0.49, 0.54, 0.36, 0.36, 0.71, 0.35, 0.64, 0.85, 0.55, 0.59, 0.29, 0.75, 0.46, 0.46, 0.60, 0.60, 0.36, 0.52, 0.68, 0.80, 0.55, 0.84, 0.34, 0.34, 0.70, 0.49, 0.56, 0.71, 0.61, 0.57, 0.73, 0.75, 0.44, 0.44, 0.81, 0.80, 0.87, 0.29, 0.50.

Table 5 presents the summary statistics for the two datasets. The analysis reveals that all datasets exhibit platykurtic distributions. Notably, Dataset I demonstrates positive skewness, whereas Dataset II displays negative skewness. These findings align with the PDF shape of the TLRK model illustrated in Figure 1, confirming its suitability for modelling such data characteristics.

Table 5. Some descriptive measures of considered datasets.

Data	n	Minimum	Maximum	Mean	Standard Deviation	Skewness	Kurtosis
I	58	0.1000	0.9900	0.3891	0.3141	0.3435	1.6568
II	50	0.2900	0.8700	0.5908	0.1615	-0.0976	2.0899

Tables 6 and 7 present the ML estimates, their associated standard errors (SEs), discrimination criteria

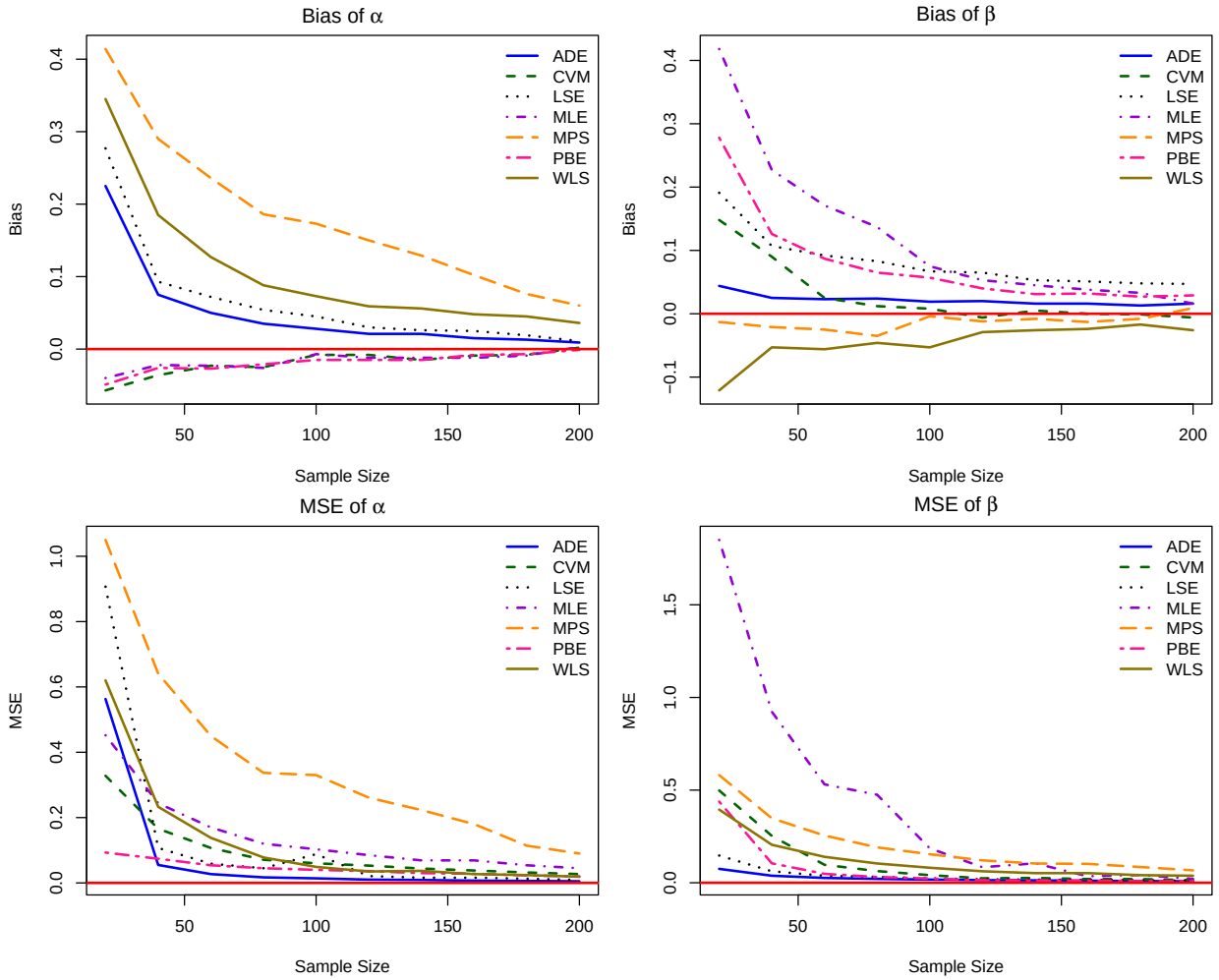

Figure 4. The bias and MSE values of the TLRK distribution for varying n when $(\alpha = 0.8, \beta = 1.5)$.

and goodness-of-fit statistics for the competing models fitted to both datasets. A careful examination of the Tables shows that the TLRK model attains comparatively lower values of discrimination criteria (ℓ, AIC, BIC, CAIC, and HQIC) relative to the competing distributions, indicating a favourable fit under likelihood-based measures. In addition, the goodness-of-fit statistics, including the W*, A*, and KS measures, suggest that the TLRK distribution provides an adequate representation of the data, with values that are the smallest among the competing models.

Figures 8 to 14 illustrate the graphical assessments, including fitted densities, CDFs, quantile-quantile (QQ), and probability-probability (PP) plots; to further support the analytical results presented in Tables 6 and 7 respectively. From the Figures, the following observations can be made for the both datasets:

- Figure 8 (Fitted PDFs). The TLRK density curve (solid black) follows the empirical histogram more closely than competing models. For Dataset I (left), TLRK captures the right-skewed concentration below 0.4; for Dataset II (right), it matches the near-symmetric peak near 0.6. This aligns with TLRK's adequate fit for the datasets.
- Figure 9 (Fitted CDFs, Dataset I). The TLRK CDF shows minimal vertical deviation from the empir-

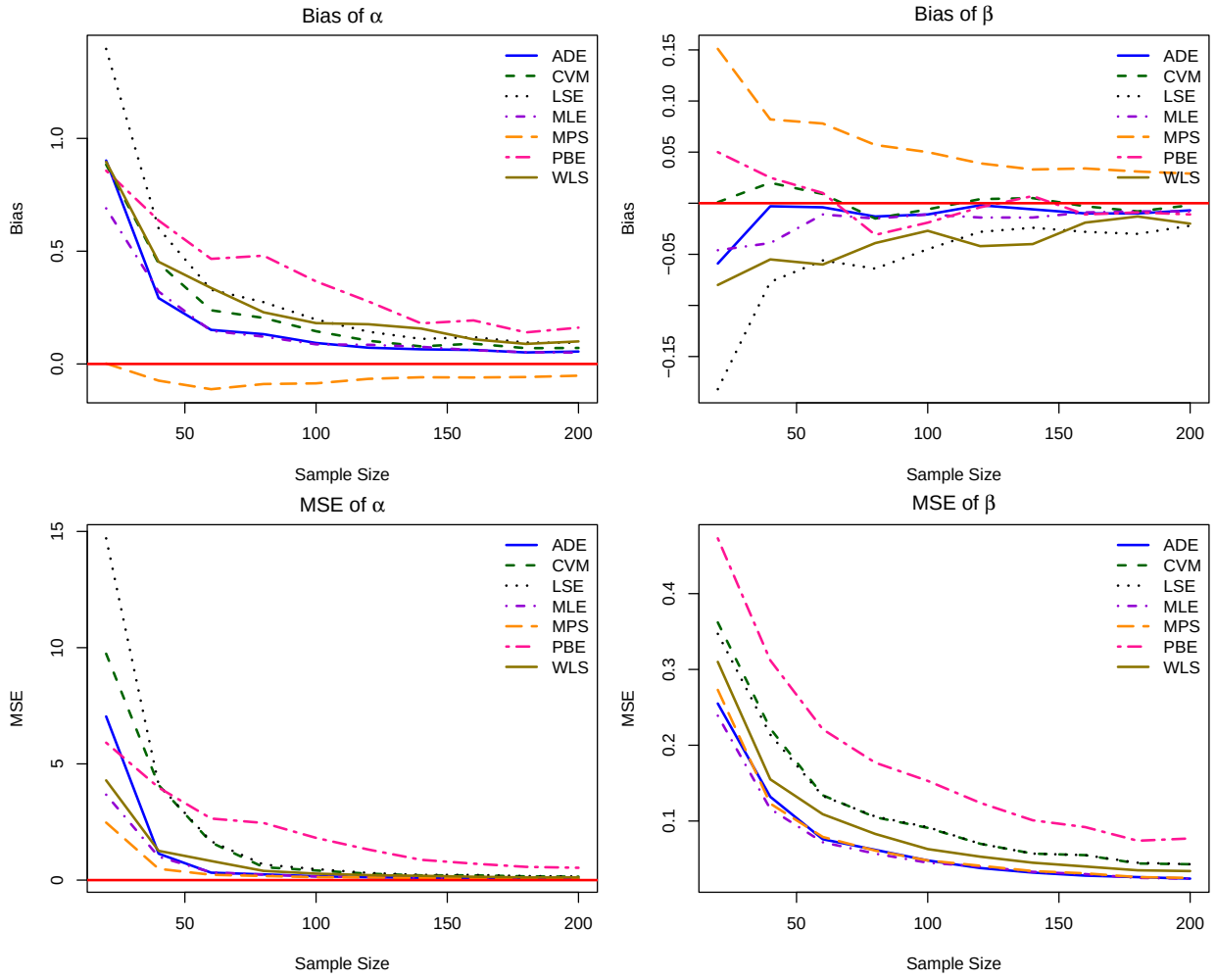

Figure 5. The bias and MSE values of the TLRK distribution for varying n when $(\alpha = 2.5, \beta = 1.2)$.

ical steps. This corresponds to TLRK's smallest KS statistic (0.0927) and highest p-value (0.701) in Table 6.

- Figure 10 (Fitted CDFs, Dataset II). TLRK exhibits good alignment with the empirical CDF across the entire support. RK shows notable divergence, consistent with RK's larger KS statistic (0.3946) and lower p-value (0.091) in Table 7.
- Figure 11 (QQ plots, Dataset I). The TLRK's points cluster closely around the diagonal with no systematic curvature. This supports TLRK's lower W* (0.0517) and A* (0.3613) in Table 6; declaring adequate quantile fit.
- Figure 12 (QQ plots, Dataset II). TLRK demonstrates excellent linearity across all quantiles. These patterns validate TLRK's lower W* (0.0537) and A* (0.3833) in Table 7; confirming strong agreement between empirical and theoretical quantiles.
- Figure 13 (PP plots, Dataset I). Most points of the TLRK fall within a narrower band around the diagonal when compared to the competing models, confirming TLRK's favourable fit as reflected in its lowest selection criteria in Table 6.

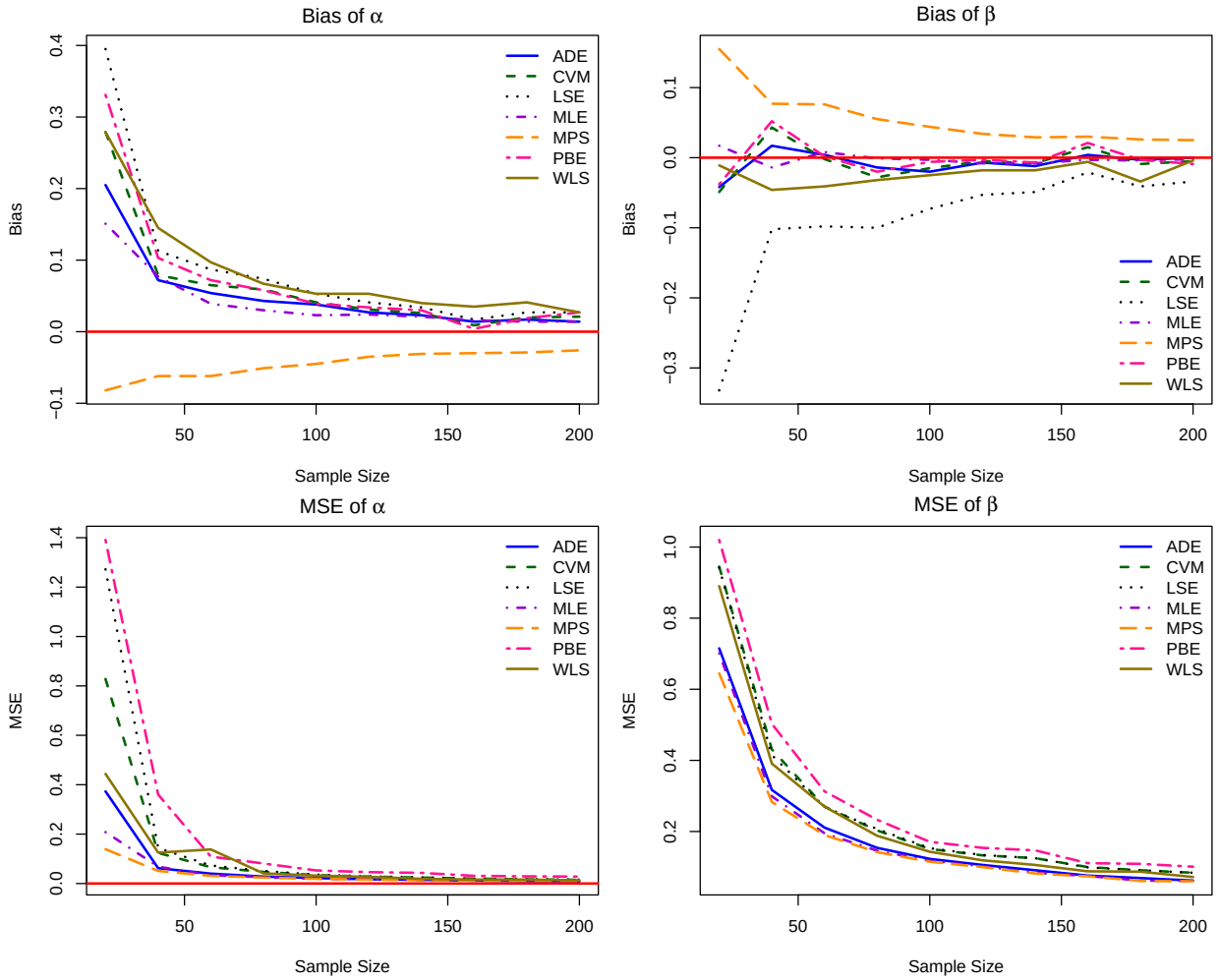

Figure 6. The bias and MSE values of the TLRK distribution for varying n when $(\alpha = 1.4, \beta = 2.7)$.

- Figure 14 (PP plots, Dataset II). The TLRK's points lie very tightly along the reference line; RK shows monotonic deviation. This graphical evidence affirms strong agreement between empirical and theoretical probabilities, consistent with its performance measures in Table 7.

To identify the optimal estimators for the datasets, multiple estimation techniques were employed, and the results are summarized in Table 8. While all methods demonstrate satisfactory performance across the datasets, a comparative analysis reveals distinct preferences:

- **Dataset I:** The WLSE method outperforms other approaches, with CVME and LSE ranking second and third, respectively.
- **Dataset II:** The WLSE method again emerges as optimal, followed by LSE, with PBE and CVME showing competitive but slightly inferior results.

The WLSE method demonstrated particular robustness, achieving top performance for the two datasets. All estimation techniques proved viable, with relative performance varying by dataset characteristics.

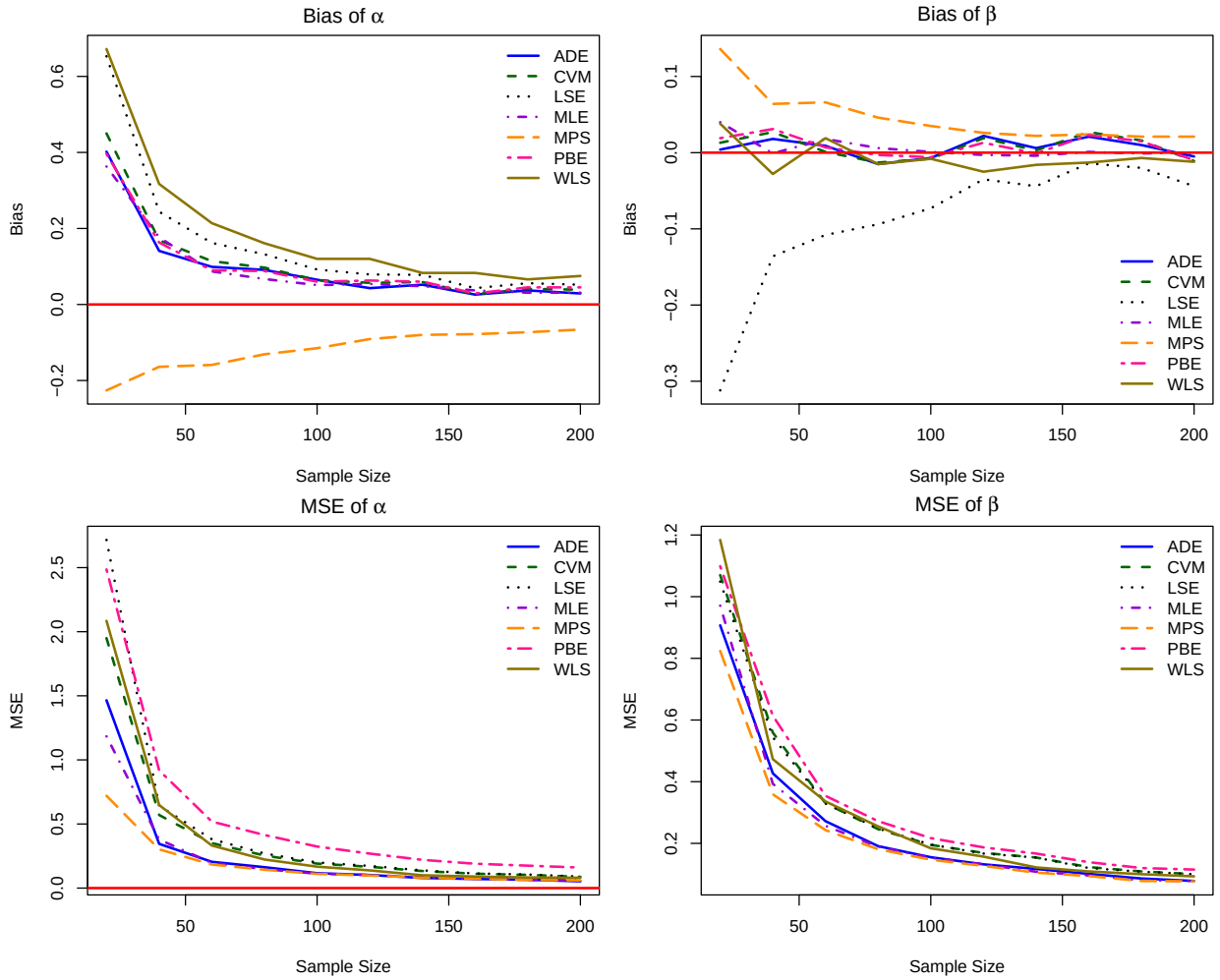

Figure 7. The bias and MSE values of the TLRK distribution for varying n when $(\alpha = 3.7, \beta = 3.3)$.

Table 6. MLEs, SEs (in parenthesis) and Performance Measures for Dataset I.

Model	$\hat{\alpha}$ (SE)	$\hat{\beta}$ (SE)	$-\hat{\ell}$	AIC	BIC	CAIC	HQIC	W*	A*	KS (p-value)
ERK	0.4573 0.0436)	1.2541 (0.1772)	-3.3609	-2.7218	1.399	-2.5037	-1.1167	0.0776	0.5894	0.1024 (0.5768)
ExRK	0.4450 (0.0440)	1.5222 (0.2023)	-4.6566	-5.3131	-1.1923	-5.0950	-3.7080	0.0616	0.4706	0.0974 (0.6411)
MORK	0.4786 (0.0415)	1.1328 (0.2526)	-2.2934	-0.5869	3.5340	-0.3687	1.0183	0.0927	0.7013	0.0947 (0.6762)
RK	0.4817 (0.0410)	-	-2.1460	-2.2919	-0.2315	-2.2205	-1.4893	0.0882	0.6730	0.1077 (0.5113)
TLRK	0.2985 (0.0326)	3.3785 (0.5194)	-6.3462	-8.6923	-4.5714	-8.4741	-7.0871	0.0517	0.3613	0.0927 (0.7014)

Table 7. MLEs, SEs (in parenthesis) and Performance Measures for Dataset II.

Model	$\hat{\alpha}$ (SE)	$\hat{\beta}$ (SE)	$-\hat{\ell}$	AIC	BIC	CAIC	HQIC	W*	A*	KS (p-value)
ERK	0.8901 (0.0719)	2.9035 (0.4108)	-21.2876	-38.5751	-34.7511	-38.3198	-37.1189	0.0899	0.5829	0.1239 (0.4261)
ExRK	0.8622 (0.0725)	3.4312 (0.4421)	-21.8974	-39.7948	-35.9708	-39.5395	-38.3386	0.0697	0.4698	0.1061 (0.6269)
MORK	0.9608 (0.0732)	3.9833 (0.9925)	-17.0868	-30.1736	-26.3496	-29.9183	-28.7174	0.2019	1.2321	0.1218 (0.4482)
RK	0.8803 (0.0754)	-	-0.8924	0.2152	2.1272	0.2986	0.9433	0.1180	0.7439	0.3946 (0.0000)
TLRK	0.5930 (0.0537)	8.8208 (1.2478)	-22.3099	-40.6198	-36.7958	-40.3645	-39.1636	0.0537	0.3833	0.0911 (0.8013)

Table 8. Estimations and Goodness-of-fit for the Datasets.

Method	Dataset I				Dataset II			
	$\hat{\alpha}$	$\hat{\beta}$	KS	p-value	$\hat{\alpha}$	$\hat{\beta}$	KS	p-value
ADE	0.3024	3.1584	0.0724	0.9214	0.5665	8.3527	0.0834	0.8780
CVME	0.2932	3.1559	0.0634	0.9740	0.5697	8.2119	0.0762	0.9333
LSE	0.2969	3.0469	0.0640	0.9716	0.5764	7.9803	0.0716	0.9599
MPSE	0.2693	3.9216	0.1174	0.4011	0.5300	9.2376	0.1336	0.3339
PBE	0.3027	3.1085	0.0669	0.9576	0.5857	8.3630	0.0759	0.9356
WLSE	0.3069	3.0220	0.0628	0.9760	0.5672	8.0217	0.0694	0.9697

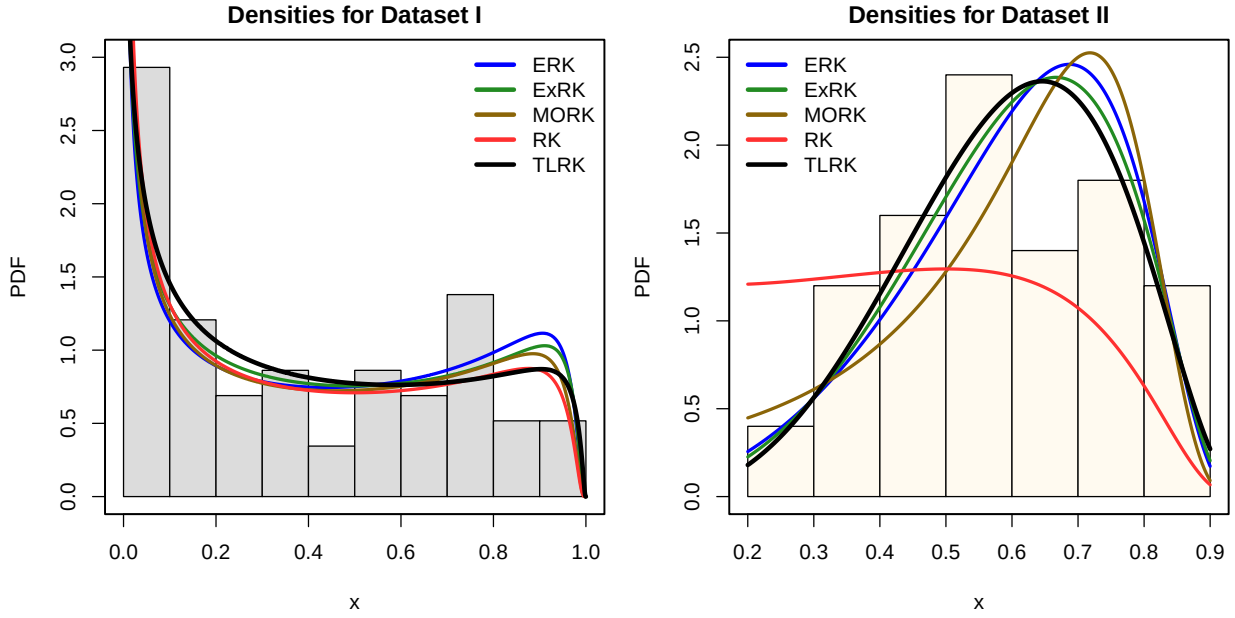

Figure 8. The Fitted PDFs for Datasets I and II.

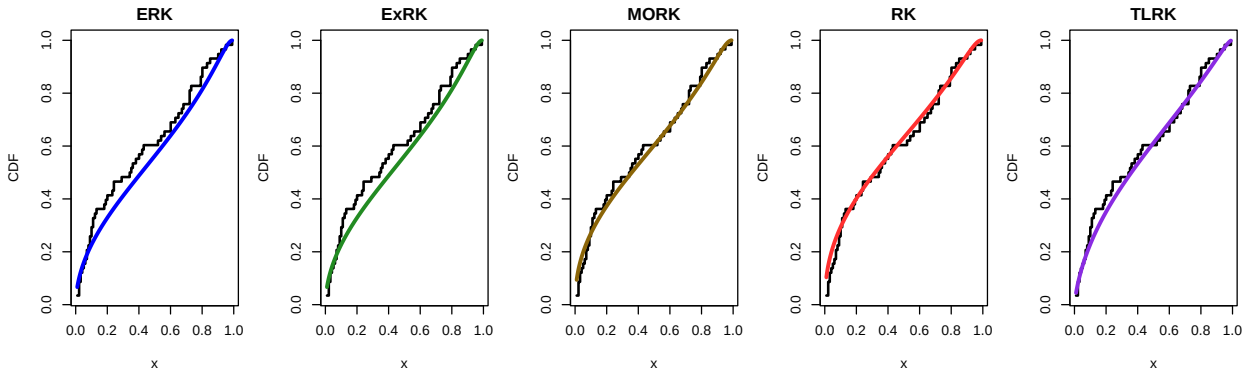

Figure 9. The Fitted CDFs for Dataset I.

7. Conclusion

This study introduces the Topp-Leone Reduced Kies distribution, a novel member of the Topp-Leone-G family of distributions. Analysis of the probability density function plots demonstrates the model's capa-

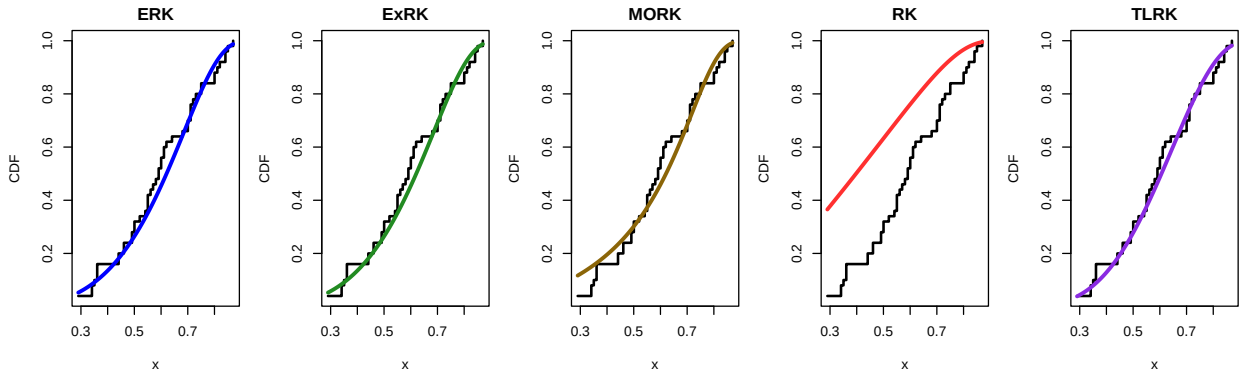

Figure 10. The Fitted CDFs for Dataset II.

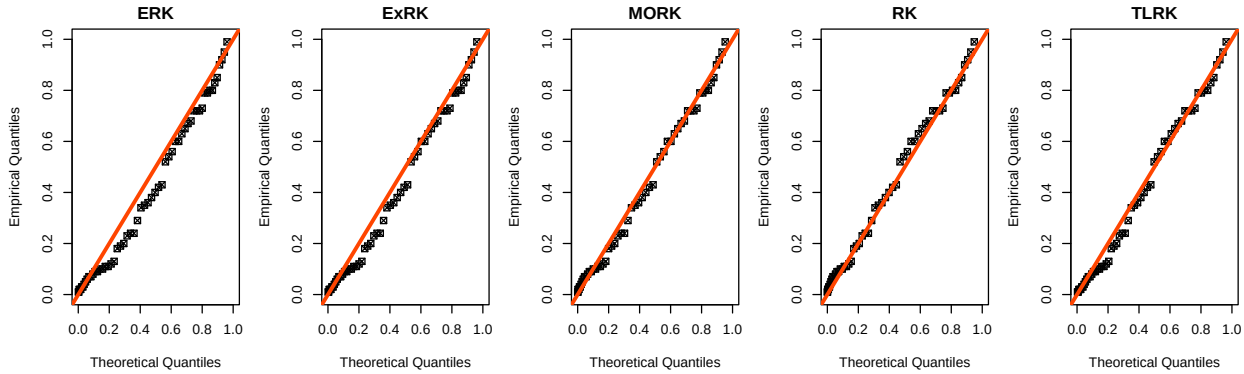

Figure 11. The QQ Plots for Dataset I.

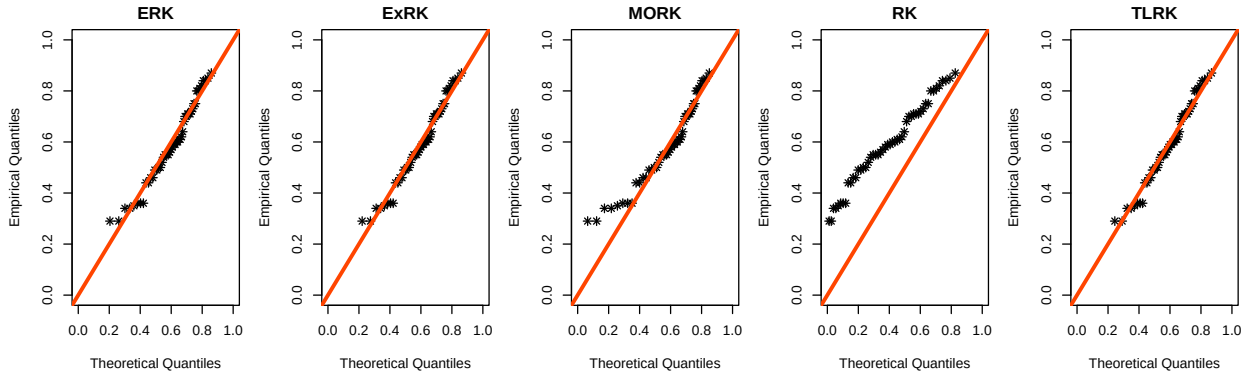

Figure 12. The QQ Plots for Dataset II.

bility to characterize unit interval data exhibiting decreasing (L-shaped), left-skewed, right-skewed, and near-symmetric distributions. Several key distributional properties were rigorously derived and examined. Notably, the hazard rate function was found to accommodate diverse failure patterns, including increasing and bathtub-shaped hazard rates. The model parameters were estimated using seven distinct estimation methodologies. A comprehensive Monte Carlo simulation study, conducted across different parameter settings and varying sample sizes, evaluated estimator performance using multiple statistical criteria. The empirical investigation employed two real datasets to assess the model's flexibility. The empirical results indicate that the proposed model achieves favourable performance relative to some existing generalisations

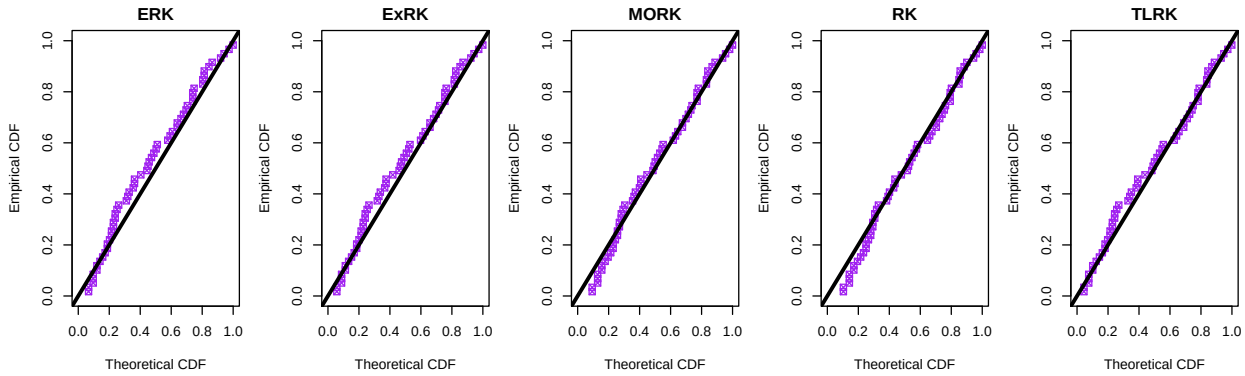

Figure 13. The PP Plots for Dataset I.

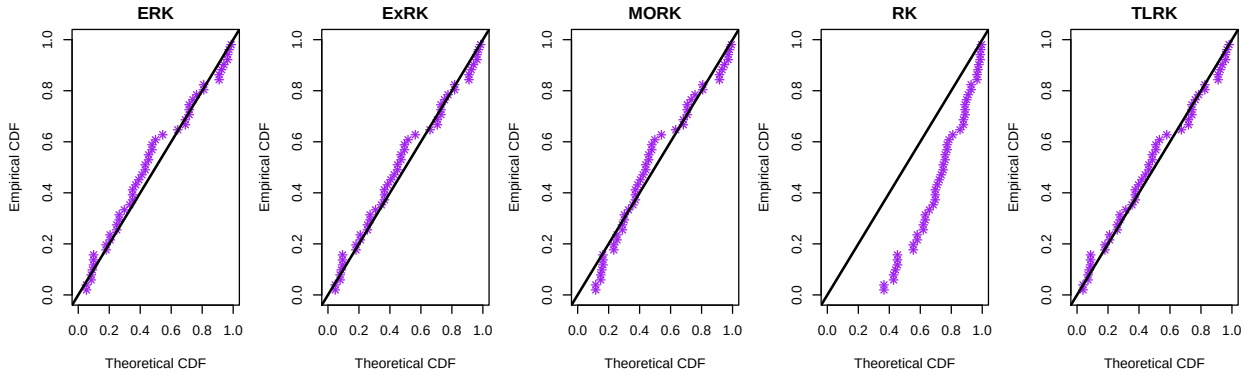

Figure 14. The PP Plots for Dataset II.

of the Reduced Kies distribution across the evaluated scenarios, thus, it offers a reliable alternative with strong adaptability to varying unit interval data. Despite its flexibility, the proposed TLRK distribution is limited to data defined on the unit interval, which restricts its applicability to bounded datasets. In addition, the estimation procedures rely on numerical optimisation, which may encounter convergence issues for certain parameter configurations or small sample sizes; and also, the current formulation does not accommodate covariate effects, limiting its use in regression settings. However, several extensions of the present work are possible. Future research may extend the TLRK model to accommodate censored data, and explore Bayesian inference with informative priors to improve estimation precision for small samples. Further generalisations incorporating additional shape parameters could also enhance modelling flexibility for multimodal or highly skewed data. In addition, a bivariate or multivariate version of the model could be developed for modelling correlated unit-interval outcomes. Finally, a regression model based on the model would be valuable for modelling bounded response variables with covariates.

Data Availability Statement

All data are provided within the article.

Conflicts of Interest

The author declares no conflict of interest.

Funding

This research received no external funding.

References

1.Abd El-Raheem, A. M., Almetwally, E. M., Mohamed, M. S., and Hafez, E. H. (2021). Accelerated life tests for modified kies exponential lifetime distribution: Binomial removal, transformers turn insulation application and numerical results. *AIMS Mathematics*, 6(5):5222–5255.

2.Afify, A. Z., Nassar, M., Kumar, D., and Cordeiro, G. M. (2022). A new unit distribution: Properties, inference, and applications. *Electronic Journal of Applied Statistical Analysis*, 15(2):460–484.

3.Al-Shomrani, A., Arif, O., Shawky, K., Hanif, S., and Shahbaz, M. Q. (2016). Topp-leone family of distributions: Some properties and application. *Pakistan Journal of Statistics and Operation Research*, 12(3):443–451.

4.Alam, I., Ahmed, A., and Ali, I. (2024). Estimation of maintenance costs under partially accelerated life tests with multiply censoring for reduced kies distribution. *Thailand Statistician*, 22(1):202–218.

5.Almuqrin, M. A., Gemeay, A. M., Abd El-Raouf, M. M., Kilai, M., Aldallal, R., and Hussam, E. (2022). A flexible extension of reduced kies distribution: Properties, inference, and applications in biology. *Complexity*, 2022:6078567.

6.Anderson, T. W. and Darling, D. A. (1952). Asymptotic theory of certain "goodness-of-fit" criteria based on stochastic processes. *The Annals of Mathematical Statistics*, 23(2):193–212.

7.Bakr, M. E., Al-Babtain, A. A., Mahmood, Z., Aldallal, R., Khosa, S. K., Abd El-Raouf, M. M., Hussam, E., and Gemeay, A. M. (2022). Statistical modelling for a new family of generalized distributions with real data applications. *Mathematical Biosciences and Engineering*, 19(9):8705–8740.

8.Bandar, S. A., Hussein, E. A., Yousof, H. M., Afify, A. Z., and Abdellatif, A. D. (2023). A novel extension of the reduced-kies family: Properties, inference, and applications to reliability engineering data. *Advances in Mathematical Modeling and Applications*, 8(1).

9.Bashiru, S. O., Isa, A. M., Khalaf, A. A., Khaleel, M. A., Arum, K. C., and Anioke, C. L. (2025). A hybrid cosine inverse lomax-g family of distributions with applications in medical and engineering data. *Nigerian Journal of Technological Development*, 22(1):261–278.

10.Bourguignon, M., Silva, R. B., and Cordeiro, G. M. (2014). The weibull-g family of probability distributions. *Journal of Data Science*, 12(1):53–68.

11.Choi, K. and Bulgren, W. G. (1968). An estimation procedure for mixtures of distributions. *Journal of the Royal Statistical Society: Series B (Methodological)*, 30(3):444–460.

12.Cordeiro, G. M. and de Castro, M. (2011). A new family of generalized distributions. *Journal of Statistical Computation and Simulation*, 81(7):883–898.

13.Dey, S., Nassar, M., and Kumar, D. (2019). Moments and estimation of reduced kies distribution based on progressive type-ii right censored order statistics. *Hacettepe Journal of Mathematics and Statistics*, 48(1):332–350.

14.Ehizojie, E. E. (2025). The exponentiated generalized reduced kies distribution with properties and applications on burr measurement datasets. *Malaysian Journal of Science and Advanced Technology*, 5(4):320–331.

15.Ehizojie, E. E. (2026). The alpha power reduced kies distribution: Properties, estimation techniques, and applications to insurance and dairy datasets. *Journal of Statistical Sciences and Computational Intelligence*, 2(2):406–423.

16.Eugene, N., Lee, C., and Famoye, F. (2002). Beta-normal distribution and its applications. *Communications in Statistics - Theory and Methods*, 31(4):497–512.

17.Fisher, R. A. (1922). On the mathematical foundations of theoretical statistics. *Philosophical Transactions of the Royal Society of London. Series A, Containing Papers of a Mathematical or Physical Character*, 222(594-604):309–368.

18.Gupta, R. D. and Kundu, D. (2001). Exponentiated exponential family: An alternative to gamma and weibull distributions. *Biometrical Journal*, 43(1):117–130.

19.Haruna, I., Zakari, Y., Abdullahi, U. K., David, R. O., and Falgore, J. Y. (2025). On the study of kumaraswamy reduced kies distribution: Properties and applications. *Communications in Physical Sciences*, 12(2):1036–1060.

20.Ibrahim, A. L. I., I. A. M. B. S. O. and Chinedu, A. K. (2025). Cosine kumaraswamy family of ditsributions: Properties and applications to real-world datasets. *Sigma*, 43(6):2185–2196.

21.Kao, J. H. K. (1958). Computer methods for estimating weibull parameters in reliability studies. *IRE Transactions on Reliability and Quality Control*, RQC-7:15–22.

22.Kao, J. H. K. (1959). A graphical estimation of mixed weibull parameters in life-testing of electron tubes. *Technometrics*, 1(4):389–407.

23.Kenney, J. F. and Keeping, E. S. (1962). *Mathematics of statistics*, volume 1. D. Van Nostrand Company, 3rd edition.

24.Kies, J. A. (1958). The strength of glass. Technical Report NRL Report 5098, Naval Research Laboratory.

25.Kumar, C. S. and Dharmaja, S. H. (2013). On reduced kies distribution. In *Collection of recent statistical methods and applications*, pages 111–123. Department of Statistics, University of Kerala.

26.Kumar, C. S. and Dharmaja, S. H. (2017). The exponentiated reduced kies distribution: Properties and applications. *Communications in Statistics - Theory and Methods*, 46(17):8778–8790.

27.Moors, J. J. A. (1988). A quantile alternative for kurtosis. *The Statistician*, 37(1):25–32.

28.Mushtaq, A., Kayid, M., and Alomani, G. (2025). A new discrete generalized class of distribution with application to radiation and covid-19 data. *Journal of Radiation Research and Applied Sciences*, 18(2):101485.

29.Park, J. H., Lee, D. K., Kang, H., Kim, J. H., Nahm, F. S., Ahn, E., In, J., Kwak, S. G., and Lim, C. Y. (2022). The principles of presenting statistical results using figures. *Korean Journal of Anesthesiology*, 75(2):139–150.

30.Sapkota, L. P., Kumar, V., Gemeay, A. M., Bakr, M. E., Balogun, O. S., and Muse, A. H. (2023). New lomax-g family of distributions: Statistical properties and applications. *AIP Advances*, 13(9):095128.

31.Sudsila, P., Thongteeraparp, A., Aryuyuen, S., and Bodhisuwan, W. (2022). The generalized distributions on the unit interval based on the t-topp-leone family of distributions. *Trends in Sciences*, 19(19):6186.

32.Sule, I., Sani, I. D., Audu, I., and Jibril, H. M. (2020). On the topp leone exponentiated-g family of distributions: Properties and applications. *Asian Journal of Probability and Statistics*, 7(1):1–15.

33.Suleiman, A. A., Daud, H., Othman, M., Ishaq, A. I., Indawati, R., Abdullah, M. L., and Husin, A. (2023). The odd beta prime-g family of probability distributions: properties and applications to engineering and environmental data. *Computer Sciences and Mathematics Forum*, 7(1):20.

34.Swain, J. J., Venkatraman, S., and Wilson, J. R. (1988). Least-squares estimation of distribution functions in johnson's translation system. *Journal of Statistical Computation and Simulation*, 29(4):271–297.

35.Tahir, M. H. and Cordeiro, G. M. (2016). Compounding of distributions: A survey and new generalized classes. *Journal of Statistical Distributions and Applications*, 3(1).

36.Usman, M., Doguwa, S. I., Dikko, H. G., Mohammed, A. S., David, R. O., and Sadiq, I. A. (2025). Development of topp-leone odd fréchet family of distribution with properties and applications. *Communication in Physical Sciences*, 12(4):1214–1226.

37.Usta, I. and Akdede, M. (2019). Bayesian estimation of the reduced kies distribution parameters. In *Proceedings book*, page 138.

38.Wingo, D. R. (1983). Maximum likelihood methods for fitting the burr xii distribution to life test data. *Biometrical Journal*, 25:77–84.

39.Zografos, K. and Balakrishnan, N. (2009). On families of beta- and generalized gamma-generated distributions and associated inference. *Statistical Methodology*, 6(4):344–362.